
Masters Theses

Student Theses and Dissertations

Spring 2016

Aspen simulation of oil shale and biomass process

Anand Alembath

Follow this and additional works at: https://scholarsmine.mst.edu/masters_theses



Part of the [Chemical Engineering Commons](#)

Department:

Recommended Citation

Alembath, Anand, "Aspen simulation of oil shale and biomass process" (2016). *Masters Theses*. 7493.
https://scholarsmine.mst.edu/masters_theses/7493

This thesis is brought to you by Scholars' Mine, a service of the Missouri S&T Library and Learning Resources. This work is protected by U. S. Copyright Law. Unauthorized use including reproduction for redistribution requires the permission of the copyright holder. For more information, please contact scholarsmine@mst.edu.

ASPEN SIMULATION OF OIL SHALE AND BIOMASS PROCESS

by

ANAND ALEMBATH

A THESIS

Presented to the Faculty of the Graduate School of the

MISSOURI UNIVERSITY OF SCIENCE AND TECHNOLOGY

In Partial Fulfillment of the Requirements for the Degree

MASTER OF SCIENCE IN CHEMICAL ENGINEERING

2016

Approved by:

**Joseph D. Smith, Advisor
Muthanna H. Al-Dahhan
Douglas Ludlow**

© 2016
Anand Alembath
All Rights Reserved

PUBLICATION THESIS OPTION

This thesis consists of the following article that has been submitted for publication as follows:

Paper I, Optimizing Reactor Parameters to Achieve Higher Process Yield in Ex-Situ Oil Shale Process has been submitted and accepted at IJCE, Recent Science.

Paper II, Multi-Zonal Modeling of Biomass Gasification Using Aspen is intended for submission to IJAF, Recent Science.

This dissertation follows formatting rules as set forth by the Missouri University of Science and Technology.

ABSTRACT

This thesis focuses on design and analysis of two major chemical processes using computer simulation which performs a steady state computation. The objective is to design processes using Aspen simulation to establish optimum operating conditions by performing various simulation runs which are challenging to execute at lab scale.

Increasing energy needs and decline of global oil prices has shifted our focus on commercially developing unconventional and renewable resources. Commercialization of any process relies on developing a process model that identifies different process parameters by performing a steady state mass and heat balance. Aspen simulation is considered an effective process modeling tool which can predict system behavior and optimize the overall process.

This thesis showcases an Aspen process model of Ex-Situ Oil Shale process and Biomass Gasification process. General approach towards design for these processes are not much different as they are thermochemical processes. This work identified the critical impact of bed temperature on crude production for oil shale process, while the impact of oxygen flow rate on temperature profile of the system and composition of syngas produced was established in biomass gasification model.

A multi-zonal kinetic based model was developed for both processes. These recommended models were designed to simulate a real system which can be modified for different operating settings and facilities. Aspen predicted values were further validated with experimental results from real systems and published data.

ACKNOWLEDGEMENT

I am forever thankful to my advisor Dr. Joseph Smith for accepting me into his massive research group. He has always given me the freedom to work on my own and has provided me with various opportunities to travel and attend conferences to showcase my research work. I consider myself lucky to work under a person who is truly altruistic. With such rewarding experience, I have no doubt in accepting that he has been the best part of my master's life.

I would like to thank Dr. Ludlow and Dr. Al-Dahhan for being a part of my thesis committee. I would like to thank my lab mate Haider Al-Rubaye for his endless support. I thank Kyle Buccheit for assisting me with Aspen. I thank Vivek Rao for teaching me CFD. I thank Hassan Golpour for his expert advice during various stages of my research. I thank other lab mates Aso, Teja, Chen, Prashant, Jeremy, Jia, Shyam, Reza, Vikram and Han for constituting a wonderful team and making this research atmosphere beautiful. I have to thank Secretary Frieda Adams who has always responded and supported well during my research period.

I have way too many names to mention here but I would like to show my thanks to my friends at 104 E, Humayun and Rajesh for making Rolla exciting. I am always grateful to my parents, my brother Amar and finally Parvathy who have backed me and helped me realize my dreams.

TABLE OF CONTENTS

PUBLICATION THESIS OPTION	iii
ABSTRACT	iv
ACKNOWLEDGEMENT	v
LIST OF ILLUSTRATIONS	ix
LIST OF TABLES	xi
NOMENCLATURE	xii
 SECTION	
1. INTRODUCTION	1
 PAPER	
I. OPTIMIZING REACTOR PARAMETERS TO ACHIEVE HIGHER PROCESS	
YIELD IN EX-SITU OIL SHALE PROCESS	
	3
ABSTRACT	3
KEYWORDS.....	4
1. INTRODUCTION	5
2. ASPEN SIMULATION	10
2.1. DRYING ZONE	10
2.2. REACTION ZONE.....	10
2.2.1. Pyrolysis Reaction	11
2.2.2. Mineral Decomposition.....	13

2.3.	SPENT SHALE RECYCLE STREAM	15
2.4.	OIL GAS RECOVERY SECTION	16
3.	SIMULATION RUN	17
3.1.	CASE 1	17
3.2.	CASE 2	19
3.3.	CASE 3	22
3.4.	CASE 4	24
4.	CONCLUSION.....	26
	REFERENCES	27
 II. MULTI-ZONAL MODELING OF BIOMASS GASIFICATION USING ASPEN SIMULATION		
	ABSTRACT	28
1.	INTRODUCTION AND BACKGROUND	29
2.	METHODOLOGY	32
2.1.	ANALYSIS OF FEED.....	32
3.	MULTIZONAL MODEL	35
3.1.	DRYING ZONE	35
3.2.	PYROLYSIS ZONE.....	36
3.3.	COMBUSTION ZONE	37
3.4.	GASIFICATION ZONE.....	38

4. ASPEN UNIT MODELS	39
5. MODEL VALIDATION, RESULTS AND DISCUSSION	46
6. CONCLUSION.....	55
REFERENCES	56
SECTION	
2. CONCLUSIONS	58
APPENDIX.....	59
VITA.....	80

LIST OF ILLUSTRATIONS

	Page
 PAPER I	
Figure 1-1: Different Samples of Oil Shale at Missouri S&T ERDC Lab. Left to right: Utah oil shale, Estonian oil shale, Jordan oil shale.....	5
Figure 1-2: Crushed Oil Shale	6
Figure 1-3: Comparison of US Oil Shale Resources with Foreign Oil Reserves	6
Figure 1-4: Stuart Shale Oil Plant	7
Figure 1-5: Paraho retort—Indirect Heating Mode	8
Figure 1-6: Modified C-SOS Model for Simulation.....	9
Figure 2-1: Aspen Simulated Model.....	16
Figure 3-1: Comparison between Production of Shale Oil, Light Gas, CO ₂ and Natural Gas Burnt.	18
Figure 3-2: CO ₂ Production from Pyrolysis and Mineral Reaction.....	19
Figure 3-3: Optimizing Flow Rate.....	20
Figure 3-4: Reactor Temperature Change with Feed Flow Rate at Fixed Heat Duty.....	21
Figure 3-5: Optimizing Temperature and Flow Rate.....	23
Figure 3-6: Optimizing Reactor Volume	25
 PAPER II	
Figure 1-1: Shares of energy sources in total global primary energy supply in 2008	29
Figure 1-2: Energy pathways for biomass	30
Figure 1-3: Down-Draft Gasifier	31
Figure 2-1: Different feed types used in Missouri S&T Energy Center lab.	33

Figure 4-1: Aspen simulation Model	39
Figure 5-1: Various Experimental Results.....	46
Figure 5-2: Aspen Model Results	47
Figure 5-3: Gas Yield with Change in Temperature.....	48
Figure 5-4: Syngas composition vs temperature for pellets.....	49
Figure 5-5: Temperature vs oxygen flow rate.....	50
Figure 5-6: Temperature profile for pellet feed	50
Figure 5-7: Syngas composition vs temperature for flakes	51
Figure 5-8: Temperature vs oxygen flow rate for flakes	52
Figure 5-9: Temperature profile for flakes feed	52
Figure 5-10: Syngas composition vs temperature for chips.....	53
Figure 5-11: Temperature vs Oxygen flow rate for chips.....	54
Figure 5-12: Temperature profile for chips	54

LIST OF TABLES

	Page
PAPER I	
Table 2-1: Elemental Analysis of Kerogen and Char [4]	11
Table 2-2: Modified Stoichiometry for the Reaction Products [8]	13
Table 2-3: Composition of Oil Shale [3]	14
PAPER II	
Table 2-1: Ultimate Analysis of Feed.....	34
Table 2-2: Proximate Analysis of Feed	34
Table 4-1 : Aspen Unit Model Description.....	40

NOMENCLATURE

<u>Symbol</u>	<u>Description</u>
mm	Millimeter
⁰ C	Degree Celsius
K	Kelvin
m ³	Cubic Meter
kg	Kilogram
g	Gram
gmol	Gram-Mole
s	Seconds
tpd	Tons per Day
BTU/hr	British Thermal Unit / Day
kJ	Kilojoules
atm	Atmospheric Pressure

SECTION

1. INTRODUCTION

This thesis is presented as two papers on oil shale pyrolysis and biomass gasification separately. Detailed literature survey on both processes has been presented in each paper. Hence in this short introduction section, the focus will be on process modeling and simulation which forms the basis for both papers.

Development and commercialization of any process requires redesign and rebuilding. Each process has multiple steps and sometimes multiple routes to reach final product. Process simulation is an important tool in process development and commercialization which helps right from screening new process to optimize existing process. According to Dow Chemicals “Process model integrates the whole organization” .A model transfers information from research to engineering to manufacturing and business team. My research goal is to design, analyze and improve the current system for two major chemical process: Oil Shale Pyrolysis and Biomass Gasification.

While modeling starts from a generic point, we then add different unit models to account for additional mechanism to make the simulation better. Depending on what effects has to be studied, different approach can considered for modeling but what is important is to target the unique aspect of any process. Key to my research is modeling an operation which constitutes different zone in which each zone is characterized by a particular process like drying, combustion, or pyrolysis .Once a model is developed, how it can be used to

further conduct sensitivity analysis, set design spec and perform a technical optimization is another important part of my research which is presented in the following two papers.

PAPER

I. OPTIMIZING REACTOR PARAMETERS TO ACHIEVE HIGHER PROCESS YIELD IN EX-SITU OIL SHALE PROCESS

ABSTRACT

Declining worldwide crude oil reserves and increasing energy needs has focused attention on developing existing unconventional fossil fuels including oil shale. America's richest oil shale deposits are found in the Green River Formation of western Colorado, eastern Utah and south-western Wyoming. The current work describes process simulation of an ex-situ oil shale pyrolysis process in a pyrolytic reactor using a novel method involving external and internal heating to increase heat transfer and mixing ratio inside the reactor.

Efforts to improve process yield for commercial operation relies on first developing a complete Aspen based process model of a proposed shale refining plant, identifying the key process parameters for the reactor and then optimizing the overall process. Simulation results are compared to earlier experimental data collected from a pilot scale rotary reactor operated by Combustion Resources, Inc. This work identified the critical impact of bed temperature on crude production in such a way that for a bed temperature of less than 400°C, results showed less than 10% conversion in crude production and for bed temperatures between 450-500°C, above 90% conversion was achieved while minimizing carbon dioxide formation from carbonate minerals inside the shale. The residence time for oil shale pyrolysis process in the reactor was also shown to be a critical parameter which

can be controlled by manipulating other key parameters like raw oil shale feed rate and also the bed temperature. The focus of this work was to optimize the rate of production of syncrude from oil shale which also enhanced process environmental and economic sustainability.

Aspen simulation of oil shale process is an effective process modeling tool to optimize the overall process. The model has kerogen, minerals and moisture combined together to define oil shale composition. The proposed model consists of three zones including drying, combustion and reactor zone which are simulated separately. Different cases are defined and studied based on various operational conditions. As a result, optimized operational values for the key parameters and also some recommendations to this process are given.

KEYWORDS

Oil shale, Optimization, Aspen, Pyrolysis, Alternative Fuel, Unconventional Hydrocarbon.

1. INTRODUCTION

Oil shale is a sedimentary rock which under a high temperature process in a very low controlled amount of oxygen called “pyrolysis” starts to devolatilize a combustible fuel gas called “synthesis gas” which further could be converted to liquid fuel or a variety of useful chemicals in a chemical refinery. Kerogen has a high hydrogen-to-carbon ratio, giving it the potential to be superior to heavy oil or coal as a source of liquid fuel [1]. Shale breaks into thin pieces with sharp edges. It occurs in a wide range of colors that include: red, brown, green, grey, and black [10]. Figure 1-1 shows different types oil shale found at Missouri S&T ERDC Lab.



Figure 1-1: Different Samples of Oil Shale at Missouri S&T ERDC Lab. Left to right: Utah oil shale, Estonian oil shale, Jordan oil shale

In ex-situ process, oil shale rocks are mined and crushed to fine particles before processing as shown in Figure 1-2.



Figure 1-2: Crushed Oil Shale [12]

Oil shale is spread across the world. United States of America has the highest deposit of oil shale which is shown in Figure 1-3. [3]. This hydrocarbon resource represents a major energy reserve and can increase U.S. energy security and support sustained economic growth.

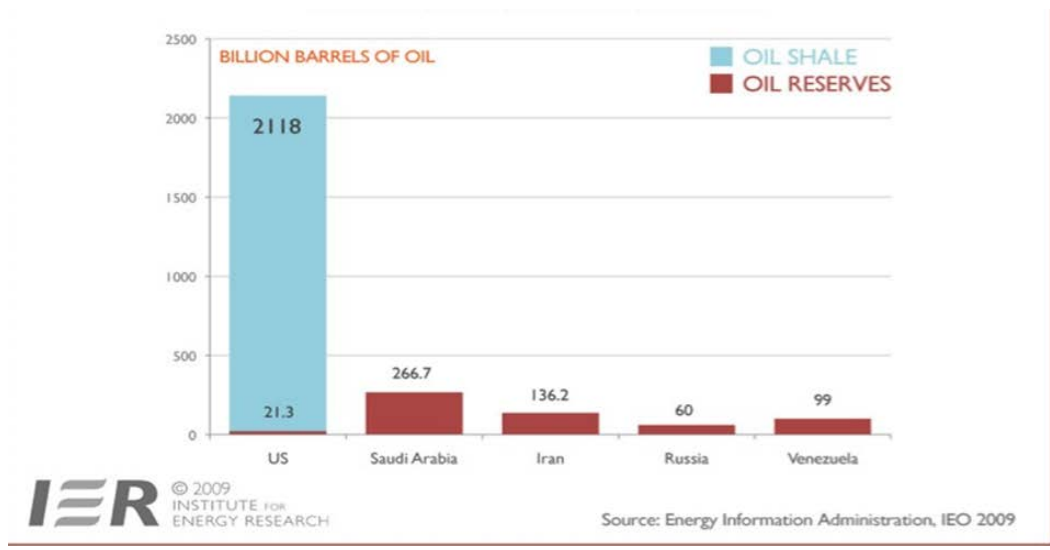


Figure 1-3: Comparison of US Oil Shale Resources with Foreign Oil Reserves [9]

Various extraction processes have been developed but none yet has been commercialized to produce synthetic crude from oil shale deposit. Australia's attempt to commercialize oil shale plant has been through the Stuart Oil Shale Project developed by Southern Pacific Petroleum NL [13]. Oil shale retort of Stuart Oil Shale plant has been shown in Figure 1-4.



Figure 1-4: Stuart Shale Oil Plant [11]

The study about how changing reactor parameters affect the overall performance of oil shale processing from Utah oil shale is based on indirectly gas-heated reactor where oil shale inside the reactor is heated through a barrier wall. Combustion chamber consists of air inlets and gas nozzles. Energy released from natural gas combustion process is transferred to reactor by convection and conduction heat transfer. In the drying zone of

reactor, crushed raw shale particles ($< 2 \text{ mm}$) are mixed with recycle stream of spent shale which act as a heat carrier. Spent shale as a by-product, is heated to ($300\text{-}600^\circ\text{C}$). The spent shale could be used as granular fill or sub-base in cement industry. [6]. In an indirectly heated reactor the heat tube is inside the case and feed is processed inside the reactor. Pilot plants are usually designed for continuous operations. Figure 1-5 shows Paraho's indirectly heated retort.

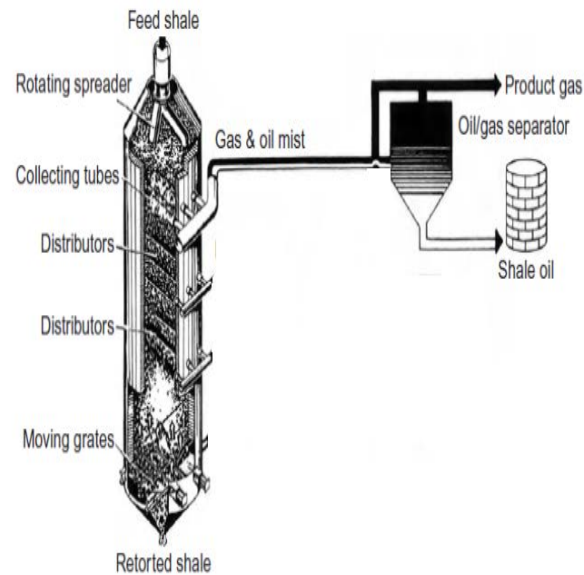


Figure 1-5: Paraho retort—Indirect Heating Mode [14]

Experimental results at the CR pilot plant concluded that the residence time decreases with increased mass flow, but not substantially.[5] Also, it was observed that having a constant heat duty from combustion resource, increasing the feed rate led to lower spent shale temperature and lower shale oil conversion percentage. [5]

The United States Government and Environmental Protection Agency (EPA) are planning to regulate high carbon dioxide tax to control green gas house emission in power plants. When the reactor is operating below a certain temperature, the release of CO₂ from carbonates for green river basin oil shale is very low[7]. Increase in the reactor temperature slightly above this specific temperature would produce significantly more CO₂, thus it is important to study how bed temperature affects the release of CO₂. CR process is known to release as low as (< 10%) carbon dioxide. CR process is called C-SOS (Clean Shale Oil Surface) Process. The flow diagram is shown in Figure 1-6.

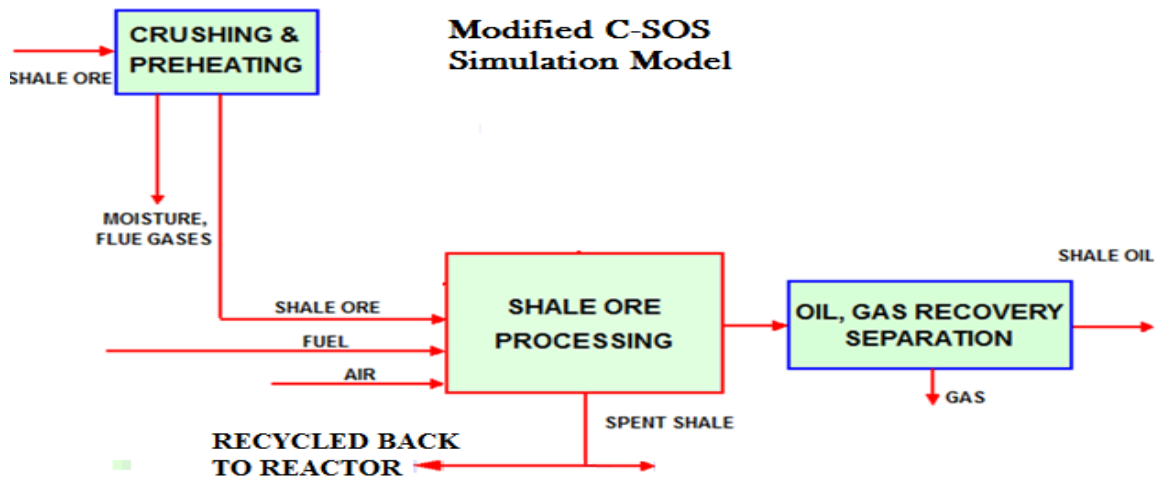


Figure 1-6: Modified C-SOS Model for Simulation

2. ASPEN SIMULATION

Aspen Simulation is used to describe the model for oil shale process and optimize the reactor parameters. Drying zone, reactor zone and the combustion zone are simulated separately and finally integrated as one model.

2.1. DRYING ZONE

Green river oil shale typically consists of 1-2% moisture by weight. Due to low moisture content, the heat duty required for drying zone is less compared to reaction zone. A heater and a separator describe the drying section with the heat duty provided from the natural gas burner. The duty from the natural gas burner is split between the drying zone and reaction zone using F-Split. The splitter ratio is set in such way that there is no moisture content in the oil shale feed stream to pyrolysis reactor.

The parameters which control the flash separation in the heater are pressure and heat duty. Pressure drop is set to zero and heat duty is controlled by natural gas consumption rate. Before entering the pyrolysis reactor, oil shale feed stream typically has a temperature range between 370 to 400 K.

2.2. REACTION ZONE

Reaction zone is the essence and core of oil shale process. Oil shale typically has 20% Hydrocarbon, 1-2% moisture and the rest consists of carbonaceous minerals. There are two kinds of reaction taking place in reaction zone. First is pyrolysis, where kerogen is converted into light gas and heavy oil. The other one is the decomposition of minerals which is a major contributor of carbon dioxide emission.

In Aspen, different types of streams can be defined. We chose to have a Mixed, Non-conventional and CI solid stream (MIXNICI). Oil shale stream is defined as a

combination of all these three streams. Moisture is defined in a Mixed Stream whereas kerogen and char as a Non-Conventional stream and minerals were introduced in a CI solid stream. Elemental composition of non-conventional components defined in Aspen is shown in Table 2-1.

Table 2-1: Elemental Analysis of Kerogen and Char [4]

	Kerogen	Char
Carbon	80.972	87.066
Hydrogen	10.193	3.069
Nitrogen	2.361	5.686
Oxygen	5.393	2.320
Sulfur	1.081	1.86

2.2.1. Pyrolysis Reaction. Using a kinetic CSTR reactor, pyrolysis reaction is modeled on the basis of Diaz and Braun model for an oil-shale retort with lift-pipe combustor.

According to the model [2]

$$R(k)=k.Fk_o.(Fk/Fk_o)^n \quad (1)$$

Where:

R (k) = kerogen reaction rate, kg/m³.s

k = rate constant, s^{-1}

Reaction constant is given as $k = 6.9 \cdot 10^{10} e^{((-21790)/T)}$, where T is in Kelvin (2)

F_{k0} = Initial kerogen concentration, kg/m^3 shale.

F_k = Final kerogen concentration, kg/m^3 shale.

n = reaction order = 1.4

The production of gas, oil, and char from kerogen pyrolysis is calculated by means of stoichiometric factors, as shown: [2]

$R = f \cdot R(k)$ (3)

f = stoichiometric factor of (kg product/ kg .s)

R = reaction rate (kg product/ $m^3 \cdot s$)

The stoichiometric factor for reaction products has been modified and presented in Table 2-2.

Table 2-2: Modified Stoichiometry for the Reaction Products [8]

Components	Stoichiometry
H ₂	0.0010
H ₂ O	0.0268
H ₂ S	0.0010
NH ₃	0.0010
CO	0.0057
CO ₂	0.0359
CH ₄	0.0142
C ₂ H ₆	0.0118
C ₃ H ₈	0.0117
C ₄ H ₁₀	0.0117
OIL	0.4767
CHAR	0.4025

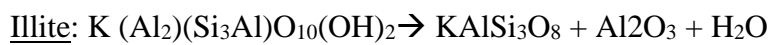
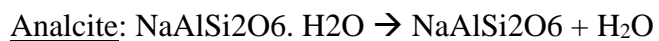
Since hydrocarbon reaction model is not pre-defined in Aspen plus, the model is written in FORTRAN subroutine developed by Aspen Technology. [8]

2.2.2. Mineral Decomposition. The Minerals considered in this model are based on the green river oil shale composition given by Brons.et al.1989 presented in Table 2-3. [3]

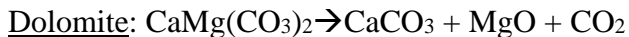
Table 2-3: Composition of Oil Shale [3]

Component	MW g/gmol	wt % Dry basis
Siderite	115.9	2.4
Dolomite	184.4	22.8
Calcite	100.1	14.1
Illite	398.3	10.9
Analcime	220.2	0.9
Dawsonite	144.0	0.6
Pyrite	120.0	1.6
Quartz	60.1	13.2
Albite	262.2	13.7
Kerogen		19.8
Total		100.0

The mineral reactions for the above inorganics defined in Table 2-3 are given as follows:



High Temperature Reactions



Mineral reactions are thermal decomposition reactions and our target is to find the temperature range at which high carbon dioxide emission occurs. To do this, we consider the mineral reactions to be thermodynamically modeled using Gibbs reactor. Reaction equilibrium is calculated based on minimizing Gibbs free energy. Both mineral and pyrolytic reactors are maintained at same temperature in each case. Using a component splitter, the products exiting the pyrolytic reactor can be separated into two streams as hydrocarbon gas and non-hydrocarbon gas which includes H_2S , NH_3 , CO and CO_2 . The HC gases are transported to a recovery section whereas the rest of gases are sent into the mineral decomposition reactor. In real process there are only two outlets coming out of the reactor 1: Gas 2, Spent shale (solid residue). In this simulation we have three outlets which include: - Hydrocarbon products, Carbon di-oxide and Spent shale solids.

2.3. SPENT SHALE RECYCLE STREAM

The energy required for pyrolysis reaction is provided by the natural gas burner. Our aim is to reduce external heat duty provided by the natural gas burners which in turn reduces the natural gas consumption and further reduces carbon dioxide emission. One approach is to recycle the spent shale back to the reactor as a heat carrier to increase heat transfer and also the mixing ratio in raw feed stream. The amount of spent shale recycled is an important factor which is very much dependent on of the feed flow rate and volume of the reaction zone.

2.4. OIL GAS RECOVERY SECTION

To extract shale oil from produced hydrocarbon gas, an oil recovery section was modeled. In this section, a flash separator is used at a temperature of 300K. The flash separator has 3 outlets: 1. Light Gas, 2. Shale Oil 3. Water

Complete process model is shown in Figure 2-1.

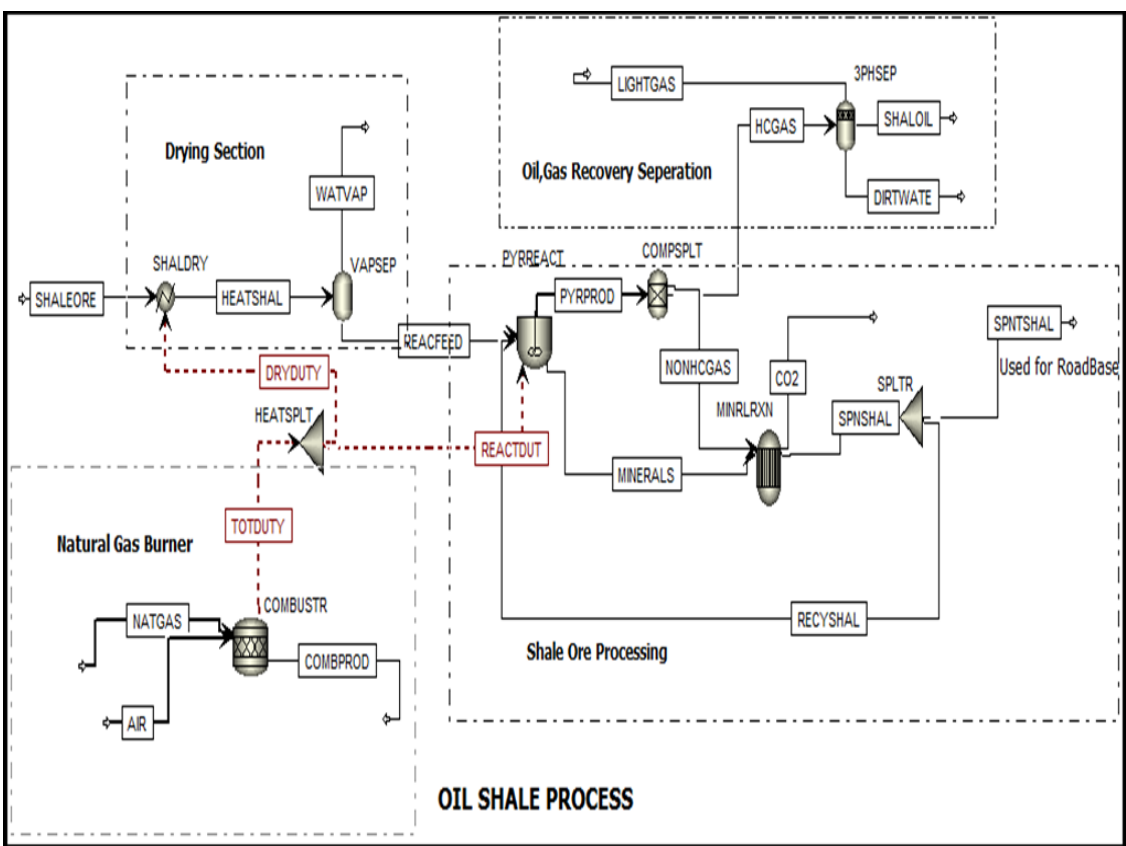


Figure 2-1: Aspen Simulated Model

3. SIMULATION RUN

3.1. CASE 1

Fixed Volume, Fixed Feed Rate, Variable Temperature

Volume of pyrolytic reactor: 0.05 m³

Feeding rate of oil shale: 26tpd

The objective of this run is to find the optimum reactor bed temperature for oil shale process. We define the optimum point here as point of maximum shale oil production and minimum carbon dioxide production. The conversion change of kerogen is between 600-873K. The temperature is varied between 600-1273K. Even though we have simulated both reactors separately, the temperatures of both reactors are at same temperature. Also heat duty required for the reactors are in direct relation with natural gas consumption. Sensitivity analysis has been done in Aspen to record the shale oil production, light gas production, natural gas consumption and carbon dioxide production from both reactors corresponding to temperature change. The values are formatted in excel and graphs are plotted as results. Pyrolysis reaction is kinetically modeled and so is a function of temperature. From Figure 3-1, it is seen that the kerogen conversion increases from 600K to 900K and becomes steady and constant after 900K.

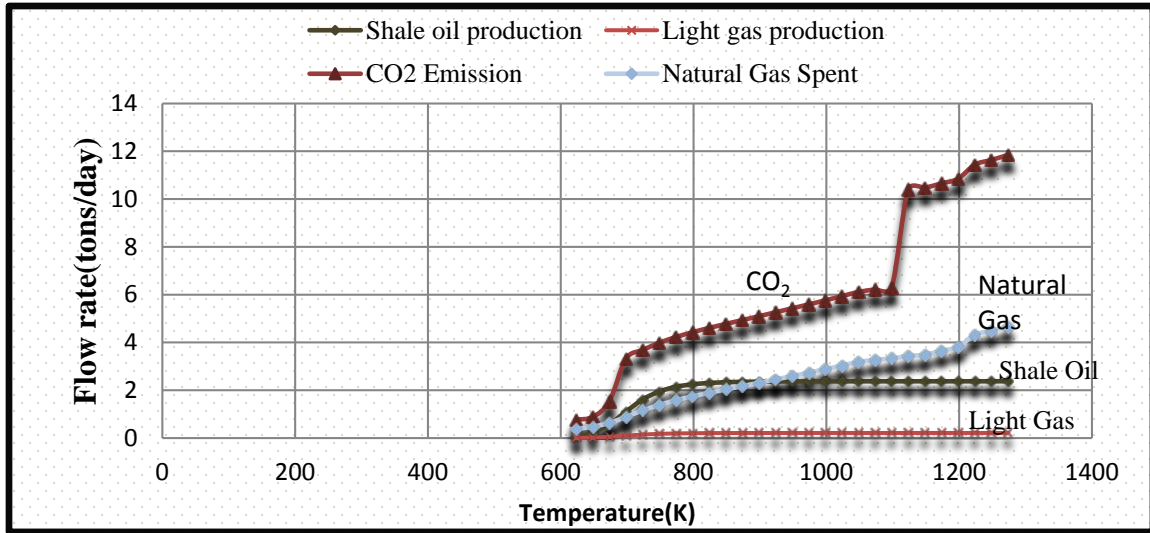


Figure 3-1: Comparison between Production of Shale Oil, Light Gas, CO₂ and Natural Gas Burnt.

Carbon dioxide production on the other hand has more critical points. The largest contribution of carbon dioxide comes from calcite and dolomite. The dolomite decomposition is said to happen at a peak temperature of 1063 K while the calcite decomposition happens between 1133-1283 K. [3]

In our model, there are two critical points for carbon dioxide emission. The graph for carbon dioxide emission from reaction zone is shown in Figure 3-2. The two critical points are at 673.15 K and 1098.15K. The first point is where the dolomite decomposition starts and 1098K is where the calcite decomposition takes place. The dolomite decomposes to calcite which further decomposes to CaO and CO₂ at 1098.15K. This is the reason why we see a sudden hike at 1123.15K.

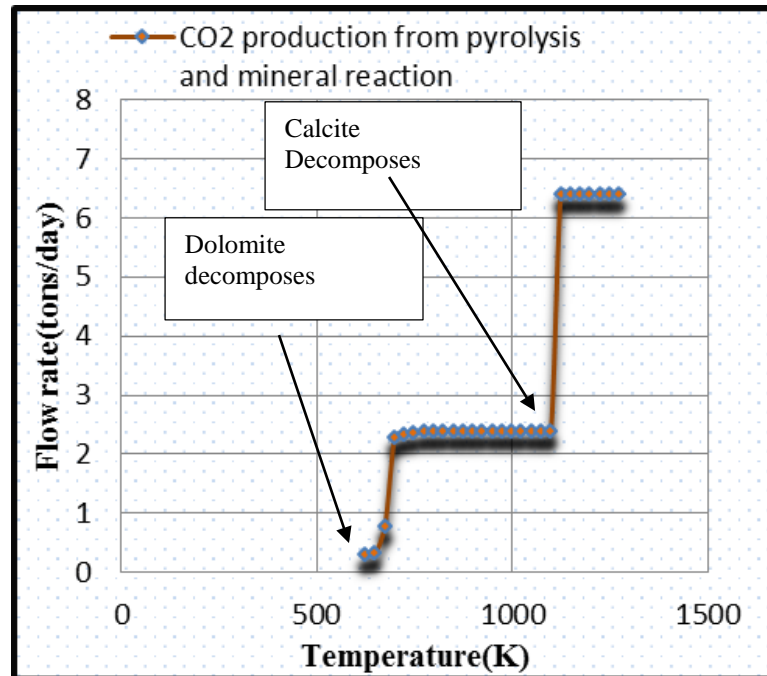


Figure 3-2: CO₂ Production from Pyrolysis and Mineral Reaction

3.2. CASE 2

Fixed Volume, Limited Heat Duty, Fixed Temperature,

Variable Feed Rate

Volume of reactor: 0.05 m³

Reactor temperature: 873K

Limited reactor heat duty: 1.46E6 Btu/hr

The objective of this run is to find the optimum feed rate for a given reactor volume. The volume is fixed as 0.05 m³ and the temperature considered to be the optimum temperature found from results of Case 1: 873K. Feed rate of raw shale is changed from 5 to 50 tpd (tons per day) with a step change of 5 tpd. As feed rate increases, residence time goes down but as far as enough heat is supplied from heating source, the conversion remains the same and shale oil production increases proportionately. This, in reality is

possible but limited. What actually happens is when we increase the feed rate, heat duty increases as well but natural gas burners has limited capacity. Based on this fact, the limit for heat duty is assumed to be $1.46E6$ BTU/hr.

Figure 3-3 indicates that the above chosen heat duty is sufficient for a feed rate of 25 tpd for reactor temperature to be maintained constant at 873 K. As feed rate goes beyond 25 tpd, the shale oil production increases accordingly if there is no constraint on heat duty. To put a constraint, now we fix the heat duty as $1.46E6$ BTU/hr and run the simulation for other flow rates.

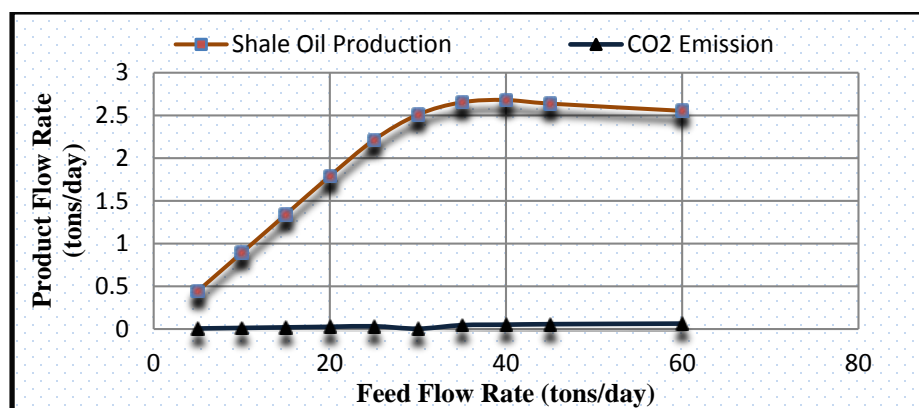


Figure 3-3: Optimizing Flow Rate

We notice a temperature drop from 873K. The important fact to be noted at this point is that both reactors have to be maintained at the same temperature. To achieve this, we record the calculated temperature for pyrolytic reactor in each run and apply this temperature on the mineral decomposition reactor. This gives us a good estimate of the CO_2 production as well. The simulation is run again to find the final shale oil and carbon

dioxide emission. When we increase the flow rate with a heat duty fixed at $1.46E6$ BTU/hr, the temperature decreases as shown in Figure 3-4.

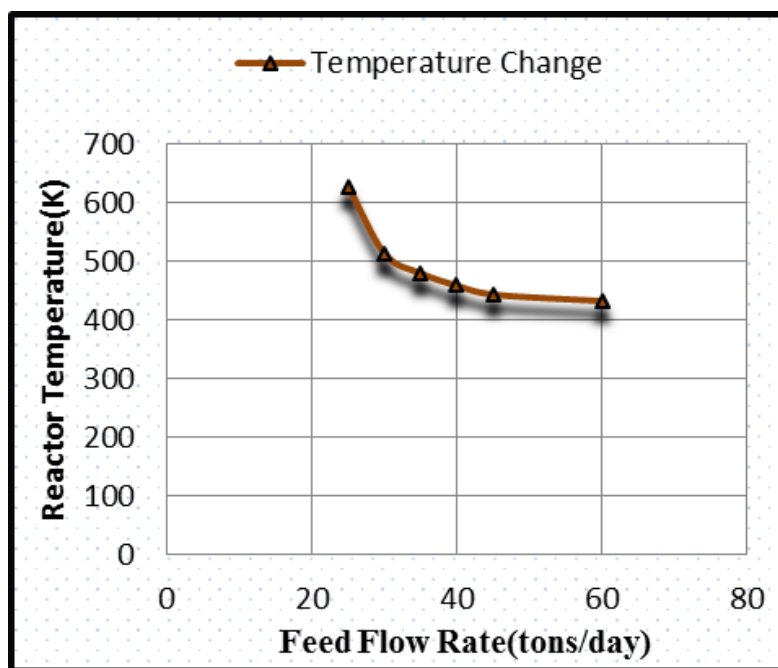


Figure 3-4: Reactor Temperature Change with Feed Flow Rate at Fixed Heat Duty

At this heat duty, the graph in Figure 3-3 indicates that above 25 tpd, the shale oil formation increases till the flow rate reaches 40 tpd above which there is a decline in the shale oil production occurring due to very low temperature (Figure 3-3).

This experimental run shows that the optimum flow rate for reactor volume of 0.05 m^3 and reactor duty of $1.46E6$ BTU/hr is 40 tpd. If the reactor temperature is maintained at 873K, the corresponding optimum flow rate is 25tpd.

Case 1 gives an optimum temperature for fixed volume and flow rate and Case 2 gives optimum flow rate for a fixed volume and temperature along with a heat duty limit.

Next is to find best combination of temperature and flow rate to maximize shale oil production which is discussed in Case 3.

3.3. CASE 3

Fixed Volume, Variable Temperature, Variable Feed Rate, Limited Heat Duty

Reactor volume: 0.05 m³

Limited reactor heat duty: 1.46E6 BTU/hr

The procedure for Case 3 is similar to Case 2 but for each single temperature we are going to run the reactor with different feed rate to find the best treatment combination of temperature and feed rate which gives us the maximum shale oil production. The graphs are plotted for different temperatures.

At 350 °C the shale oil production peaks at 0.3 tons/day (Figure 3-5(a)). This production is very low. At 400°C shale oil produced increases to 2.2 tons/day (Figure 3-5(b)). 50 degree temperature rise has an enormous increase in shale oil production but other noticeable factor is the reduction in the feed flow rate at peak point. In Figure (3-5-(a)) we found that shale oil production peaks at 100 tons/day but in Figure (3-5-(b)) the peak is seen at 80 tons/day. As the temperature increases, the shale production increases and the feed flow decreases. As emphasized above, the temperature is a crucial factor. When temperature increases, the flow rate decreases to minimize the heat duty. We could have concluded that shale oil production peaks at a point where the temperature is maximum for provided energy. Here we realize the importance of Case 1 which showed us that the maximum temperature where shale oil production can reach is 873K, above which we see a level out for a given volume and flow rate. Hence we conclude that, given an energy

constraint to the system, there is an optimum point for temperature and flow rate at which shale oil production maximizes.

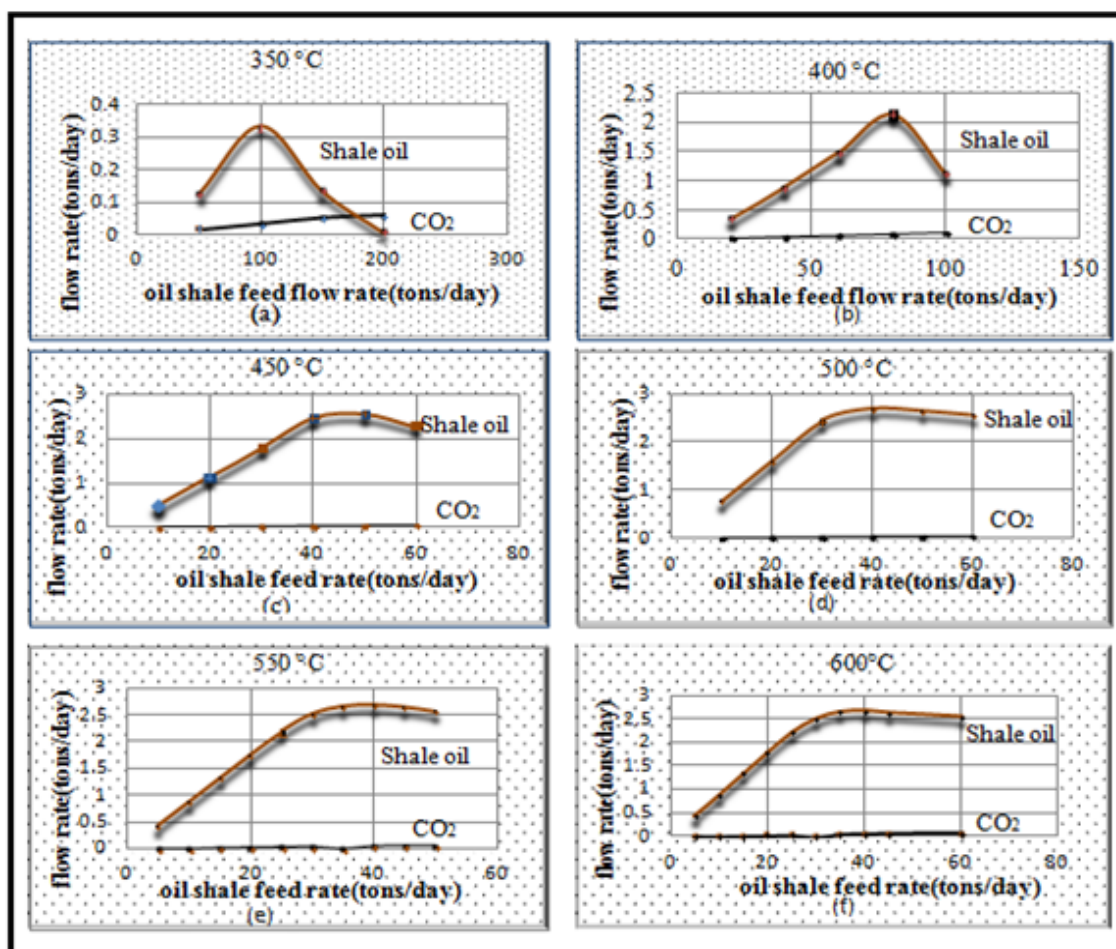


Figure 3-5: Optimizing Temperature and Flow Rate

After analyzing all the graphs, we see that the maximum shale oil production is 2.68 tpd at 40tpd shale feed rate and a temperature of 458 °C.

We conclude that for a 0.05 m³ volume reactor and a maximum heat duty of 1.46E6 BTU/hr from natural gas burner, the most optimum temperature is 458 °C and the corresponding optimum feed rate is 40 tpd.

3.4. CASE 4

Fixed optimum Temperature, Fixed optimum Feed Rate, Limited Heat Duty, Reactor Volume?

Limited reactor heat duty: 1.46E6 BTU/hr.

Flow rate: 40tpd.

The objective of Case 4 is slightly different from others. Since the reactor volume cannot be changed or be optimized once the plant is built, Case 4 is focused on designing the size of the reactor before fabrication. In a situation where we are going to build a new oil shale reactor, the most important constrain that gets fixed is supply energy. As mentioned before in previous cases, let's consider a natural gas burner which can provide a maximum heat duty of 1.46E6 BTU/hr to the reactor. Another parameter which should be in a reasonable range is the feed rate. Using results from Case 2, the feed rate is fixed at 40 tons/day. We assume that reactor is running at 450 °C .

Maximum yield and minimum volume are the desired results. The shale oil yield gradually increases as volume increases as seen Figure 3-6. Once, the heat duty limit is reached then as the volume increases, temperature decreases and obviously shale oil production does not increase significantly after this point. Comparison between Case 3 and Case 4, results show that shale oil production depends on the volume of the reactor

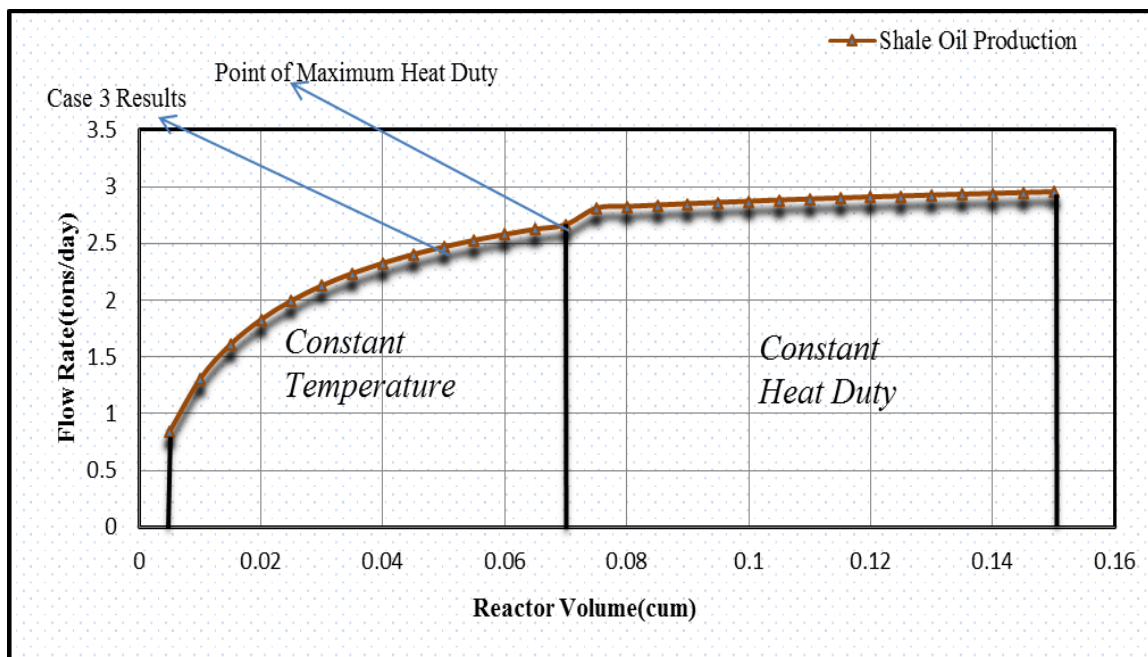


Figure 3-6: Optimizing Reactor Volume

4. CONCLUSION

The single reactor equipment has been simulated in 3 different zones separately. The model analysis tool of Aspen has been used extensively to find the optimized operating conditions. Three different cases have been studied to find the optimum operating conditions. The first case, gave us a rough estimate of best reactor bed temperature. The focus was more on temperature range of kerogen conversion and carbon dioxide formation without having a limit on heat duty. Case 1 gave a very good estimate of working temperature considering the mineral decomposition reaction. Using the Case 1 result of optimum temperature, we found out the best flow rate in Case 2. The shale oil production increases with increase in flow rate till the heat duty limit. After this point, shale oil production goes down due to decrease in temperature. This gave us the optimum flow rate for a given temperature and reactor volume. Case 3 was performed to find out the best temperature and feed rate for a given reactor volume and limited heat duty. This is the most critical sensitivity analysis and it concluded that for a 0.05 m^3 volume of reactor and $1.46 \times 10^6 \text{ BTU/hr}$ natural gas burner, the most optimum temperature is 458°C and the corresponding optimum flow rate is 40 tons/day. Another parameter which was analyzed is the reactor volume. The true significance of this analysis is felt only if it is done before setting-up the plant. Energy requirement and handling capacity for the plant is fixed. For reactor volume of 0.05 m^3 and flow rate of 40 tons/day the best yield was 2.68 tons/day of oil, but for 0.075 m^3 reactor, the shale oil yield showed to be 2.8 tons/day, a 5% increase in yield. Once the heat duty limit is reached, the percentage increase in shale oil production is not much significant with increase in volume which adds to capital cost.

REFERENCES

- [1.] Kleinberg, R. L. (2006). Oil Shale.
- [2.] Diaz, J. C., & Braun, R. L. (1984). Process simulation model for a staged, fluidized bed oil shale retort using lift pipe combustor.
- [3.] Sheritt, R., Jia, J., Meilani, P., & Schmidt, J. (2009). Advances in steady-state process modeling of oil shale retorting. 29th Oil Shale Symposium.
- [4.] Singleton, M. F., Koskinas, G. J., Burnham, A. K., & Raley, J. H. (1986). Assay Products from Green river oil shale. Lawrence Livermore National Laboratory.
- [5.] Smoot, & Douglas. (2012). Demonstration of advanced technology for surface processing of oil shale.
- [6.] Winter, M. (20001). Spent Oil Shale use in Earthwork Construction. Science Direct.
- [7.] Hendrickson, T. A. (1974). Oil shale processing methods. 7th Oil Shale Symposium.
- [8.] Aspen Plus. (2011). Model for Oil Shale Retorting Process.
- [9.] Institute for Energy Research. (n.d.). Retrieved Feb 2015, from <http://instituteeforenergyresearch.org/>:
<http://instituteeforenergyresearch.org/studies/policies-of-scarcity-in-a-land-of-plenty/>.
- [10] King, H. (2005). Geoscience News and Information. Retrieved 01 2015, from geology.com: <http://geology.com/rocks/shale.shtml>.
- [11] Crude Oil Peak. (2012, 04). Retrieved Jan 2015, from <http://crudeoilpeak.info/>:
<http://crudeoilpeak.info/proudly-powered-by-oil-shale>.
- [12] San Leon Energy. (2014, October 08). Retrieved 01 2015, from <http://www.sanleonenergy.com/>
<http://www.sanleonenergy.com/operations-and-assets/timahdit-oil-shale-bench-test.aspx>.
- [13] Stuart Oil Shale Project. (2014, August 03). Retrieved from Wikipedia:
http://en.wikipedia.org/wiki/Stuart_Oil_Shale_Project.
- [14] Speight, J. G. (2012). Shale Oil Production Processes.

II. MULTI-ZONAL MODELING OF BIOMASS GASIFICATION USING ASPEN SIMULATION

ABSTRACT

To meet the demand of increasing energy needs, our current focus is on commercially developing biomass gasification process. Efforts to improve process yield for commercial operation relies on first developing a complete Aspen based process model, identifying the key process parameters for the reactor and then optimizing the overall process. The proposed model is designed to simulate a real biomass gasification system that was designed and built here in MS&T at steady state along with a detailed modeling of all four zones in this downdraft gasifier including drying, pyrolysis, combustion and gasification zone. The model can easily be modified for different operating facilities and conditions.

The current model will analyze the following important aspects: Syngas produced, Tar present in the syngas, Equivalence ratio (air/fuel) and Temperature profile in the system. All reactors describing different processes inside the gasifier are kinetically modeled in a CSTR with surface and volumetric reactions. *ASPEN* process parameters were identified to match different operating factors and used to optimize the complete process. Results are verified with experimental yield data collected from lab scale biomass gasifier operated by Missouri S&T Energy R&D Center.

1. INTRODUCTION AND BACKGROUND

Today, the world is looking for renewable sources of energy. Global oil prices have fallen which has led to a downfall in oil & gas industry in United States. This has made us realize the importance of obtaining energy from bio-based products. Converting solid biomass into a mixture of gases which mainly consists of carbon mono-oxide and hydrogen known as syngas by thermochemical process is called biomass gasification. Recovering energy from waste by gasification process is a cost effective and reliable process and provides clean fuel. Currently biomass covers approximately 10 percent of the global energy supply [1]. Among renewable resources, the most important ones were biomass and renewable waste accounting for just under two thirds shown in Figure 1-1 (64.2 %) [2]. In 2009, 13 % of consumed biomass was used to generate heat and power, while the industries consumed 15% and transportation 4% [1].

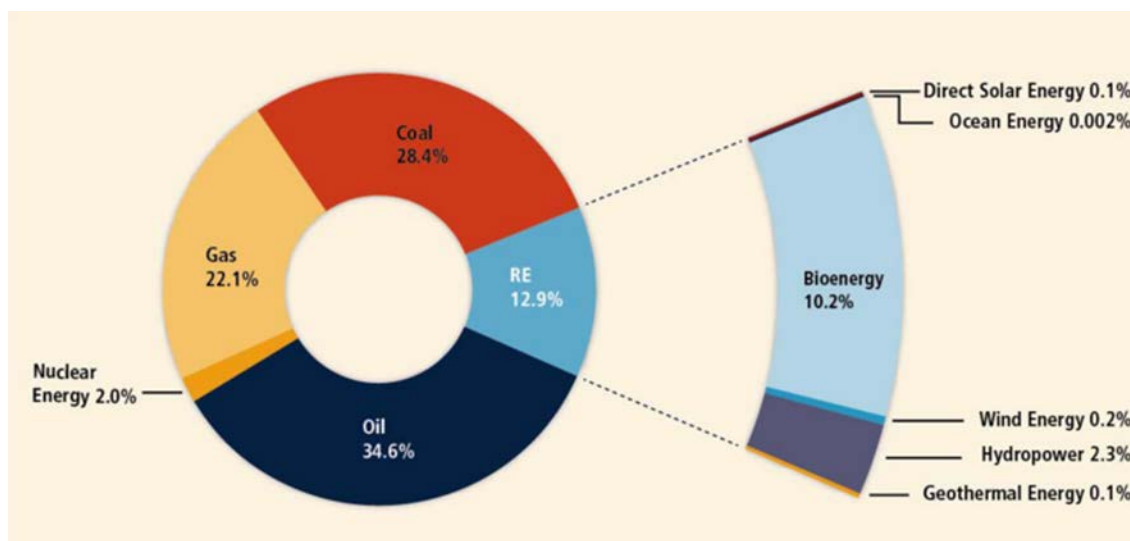


Figure 1-1: Shares of energy sources in total global primary energy supply in 2008 [3]

There are three general pathways to produce energy from biomass as shown in Figure 1-2 [4].

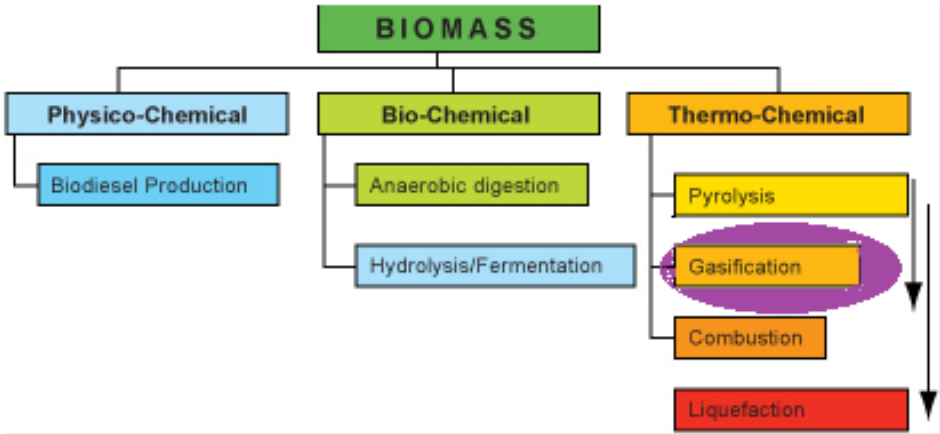


Figure 1-2: Energy pathways for biomass [4]

Our focus is on thermo-chemical process as it can handle various types of biomass. Amongst the thermo-chemical conversion technologies, biomass gasification has attracted the highest interest as it offers higher efficiencies in relation to combustion [5]. Gasification of biomass is primarily done in fixed and fluidized beds. The fixed bed gasifiers are suitable for small-scale applications. Our model is based on a fixed bed downdraft reactor which is being run at Missouri S&T. Imbert gasifier with different zones is shown in Figure 1-3.

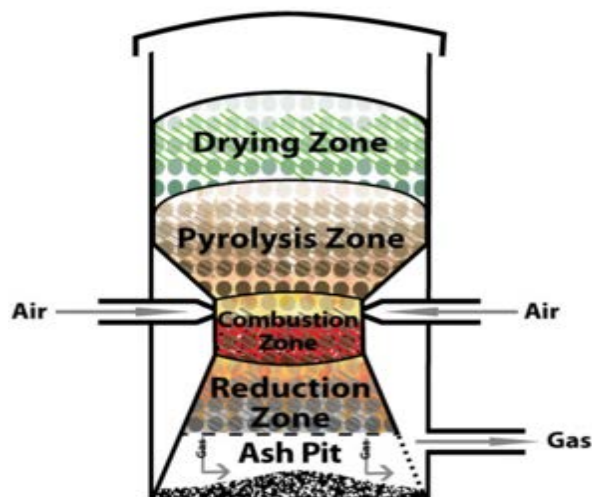


Figure 1-3: Down-Draft Gasifier [6]

Aspen Model of biomass gasifier is used to evaluate the effect of operating parameters & feed conditions. Most of the biomass gasifier models are thermodynamic equilibrium based models where Gibbs reactor is used to simulate different zones. This approach is based on Gibbs free energy minimization which is good at estimating final syngas composition but it cannot predict temperature profile across reactor. The goal of the Aspen Model developed in this work is to scale up and commercialize downdraft biomass gasification technology, therefore the multi-zonal model is based on rigorous kinetic models implemented on different zones of a biomass downdraft gasifier. This approach allows us to determine temperature profile across reactor and effect of gasification temperature on the syngas composition.

2. METHODOLOGY

Examination of biomass material properties is necessary in simulation. As fuels differ greatly in their chemical, physical and morphological properties, they have different demands in methods of gasification [7]. Depending on locality, type of wood available changes. Some factors which has to be considered are ash content, density of wood, moisture content, and amount of volatile inside the wood. High ash content can lead all ashes fuse together at high temperature. When density of a wood is higher, it has also higher energy content for the same volume.

Biomass is defined in terms of proximate and ultimate analysis. Ultimate analysis gives the elemental composition of biomass. Proximate analysis gives the volatile matter that determines the components given off at high temperature, fixed carbon which is the residue after the volatile is driven off, ash and moisture content. Proximate analysis is related to heating of biomass by relative proportions of fixed carbon (FC) and volatile matter (VM). Different proximate and ultimate analysis leads to different bulk properties such as density and heating value [8]. To study this effect, our simulation uses three different types of wood as feed materials.

2.1. ANALYSIS OF FEED

At our Missouri S&T Energy Center Lab, three types of wood were used to run the biomass gasifier which are pellets, flakes and chips as shown in Figure 2-1.



Figure 2-1: Different feed types used in Missouri S&T Energy Center lab.

Proximate and ultimate analysis for the above feeds were carried in Missouri S&T Energy Center and results are shown in Tables 2-1 and 2-2.

Table 2-1: Ultimate Analysis of Feed

<i>Feed</i>	<i>Chips</i>	<i>Flakes</i>	<i>Pellets</i>
Carbon	47.97	47.95	48.53
Hydrogen	5.85	6.11	5.52
Nitrogen	0.25	0.05	0.05
Oxygen	44.21	45.27	44.81
Ash	1.7	0.6	0.98

Table 2-2: Proximate Analysis of Feed

<i>Feed</i>	<i>Pellets</i>	<i>Flakes</i>	<i>Chips</i>
Volatile Matter	83.01	79.47	79.88
Fixed Carbon	16	19.91	18.4
Ash	0.98	0.6	1.7
Moisture	7.56	20	35.19

3. MULTIZONAL MODEL

As mentioned above the overall gasification process is simulated in four separate zones as shown in Figure 1-3. Each zone is described as follows:

3.1. DRYING ZONE

Moisture content of the feed stock is an important factor to be able to stabilize a good combustion bed while having high moisture feed and to determine if the gasifier is capable to run in a steady state condition for a long time. Also the heating value of the gas produced depends on the moisture content of the feedstock. Moisture content can be determined on a dry basis as well as on a wet basis method. In this study the dry basis method was used to calculate the moisture content as shown in equation below. The vaporization of water to steam requires a heat input of 1000 Btu/lb of water [9]. Energy which could be useful in steam production is diverted to drying the wood fuel. So high moisture content reduces the thermal efficiency and results in low heating value of produced gas. Also, in downdraft gasifiers, high moisture contents give rise to low temperatures in the combustion zone which leads to high tar formation. Moisture content is calculated using following equation:

$$\text{Moisture content} = [(\text{Wet weight} - \text{Dry weight}) / \text{Dry weight}] * 100$$

The modeling part of drying zone includes a yield reactor with a separator which removes water vapor. Free water is separated from the wet biomass. Water vapor along with dry biomass is sent to pyrolysis zone.

3.2. PYROLYSIS ZONE

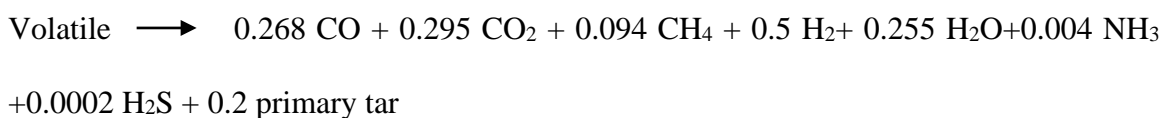
Pyrolysis is where the volatile component vaporizes to a mixture of gases (devolatilization). The volatile vapor mainly consists of hydrogen, carbon monoxide, carbon dioxide, methane, hydrocarbon gases, tar, and water vapor. As biomass has high volatile content, pyrolysis is an important step in biomass gasification. Remaining solid char and ash are also produced in this step. Primary products characterized by compounds evolved from cellulose, hemicellulose or lignin [10]. The pyrolysis zone in Aspen is modeled in 3 separate reactions:

- Devolatilization

Devolatilization is a one-step reaction modeled in a yield reactor which decomposes biomass fuels volatiles, char and ash.

- Primary pyrolysis

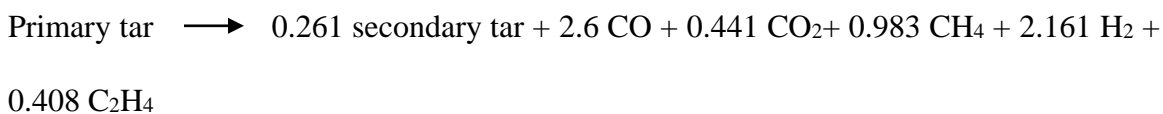
In this step, light gases are driven off along with tar from volatiles by following reaction where primary tar is defined as $C_{6.607}H_{11.454}O_{3.482}$ [11]



Rate of this reaction is given by: $R_{p1} = 4.38 \cdot 10^9 \exp(-1.527 \cdot 10^5 / RT_s) C_{\text{volatile}}$ [11]

- Secondary pyrolysis

Reaction below converts the primary tar to secondary tar and other products where secondary tar is defined to be pure benzene [11].



Reaction rate for the secondary pyrolysis is given by: $R_{p2} = 4.28 \cdot 10^6 \exp(-1.08 \cdot 10^5 / RT_g)$

$C_{\text{primary tar}}$.

3.3. COMBUSTION ZONE

Char reactions are considered unreacted shrinking core model which assumes char particles to be spherical; grains and solid-gas phase reaction takes place on the external surface [11]. Combustion reactions are modeled with 2 types of reaction:

- Char oxidation reactions



- Hydrogen combustion reaction



In downdraft gasifiers, generally air is introduced in the combustion zone which has a large volume of nitrogen. This dilutes the syngas and reduces the concentration of hydrogen (H_2) and carbon monoxide (CO), which reduce syngas heat value [12]. For this reason, in our simulation we have replaced air with oxygen which determines the product and temperature distribution of a gasification system.

Combustion zone is the zone which provides energy to endothermic pyrolysis and gasification reactions. According to Worley and Yale, heat required for pyrolysis is between 1.6-2.2 kJ/g which is equal to 6-10% of heat of combustion of dry biomass [13]. This heat is provided by combustion of char and other volatiles. For this reason, temperature at combustion zone are higher compared to other zones. Typical temperature range for combustion zone is between 950-1150°C [14]. The lower tar concentration in downdraft reactors are due to gas passing through a high temperature zone (the combustion

zone). Since the temperature in combustion zone is high, the tar cracking reaction is specified in this zone.

3.4. GASIFICATION ZONE

Gasification zone is the most critical zone in a gasifier. The hot gases and carbon burnt goes through a series of reduction reactions. Temperature in gasifier zone is less compared to combustion zone which is due to endothermic reactions. The temperature drop will depend on the extent of reactions. According to Babu & Seth as char moves downwards, char-gas reactions along with shrinking of particles leads to a decrease in char size and increase in porosity leading to more active sites and thereby increasing the conversion of char [15]. To account this mechanism, multi-phase char reaction model is written in a *FORTRAN* subroutine developed by Aspen Technology [16]. Important reduction reactions taking place in gasification zone are as follows:

Water Gas Reaction



Boudourd Reaction



Hydrogasification Reaction



Water Gas Shift Reaction



4. ASPEN UNIT MODELS

Figure 4-1 shows the complete process model developed for biomass gasification and Table 4-1 shows describes the function of each unit model used.

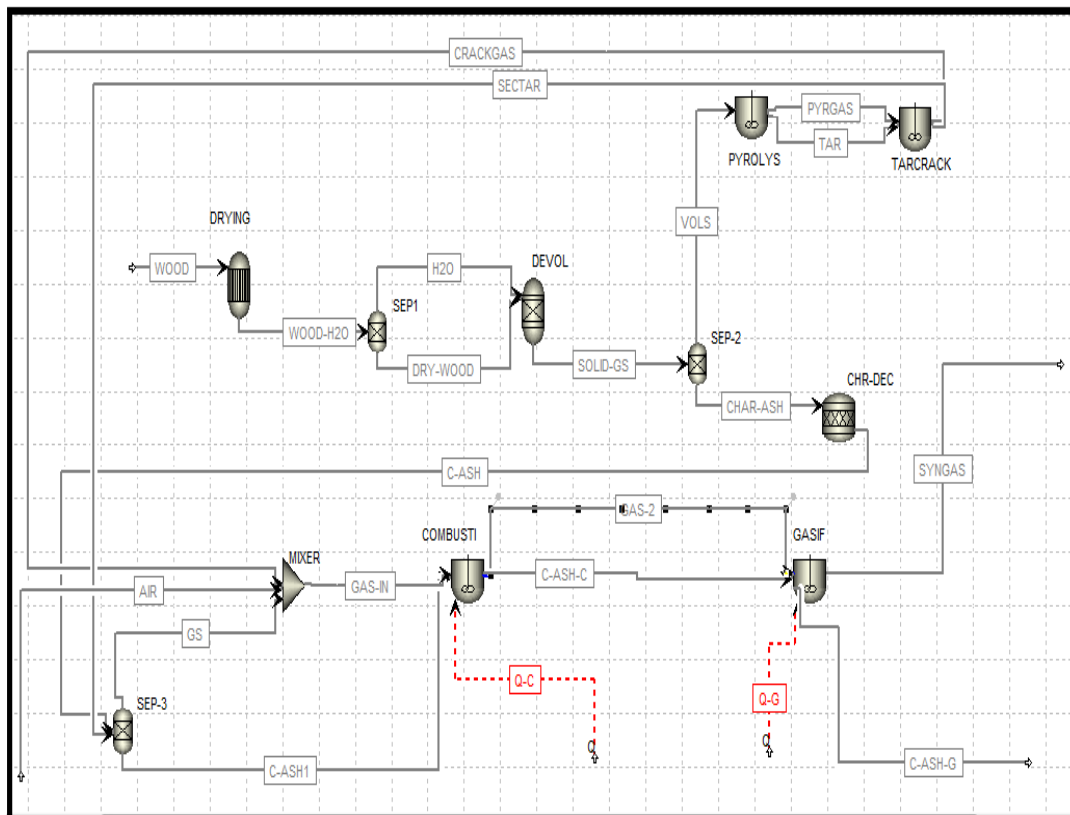


Figure 4-1: Aspen simulation Model

Table 4-1 : Aspen Unit Model Description

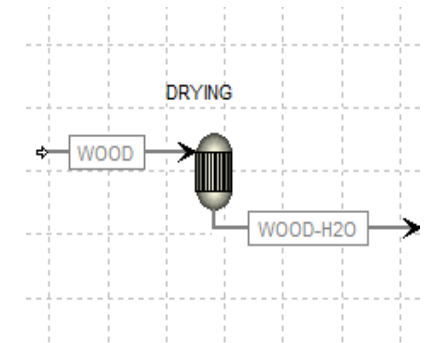
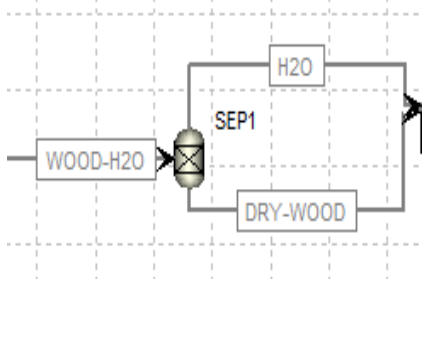
Aspen Unit Block	Function	Specification
	<p>Yield reactor removes free moisture present in biomass.</p>	<p>Temperature: 373K Pressure: 1atm Yield: water: 8% (for pellets) dry-wood: 92%</p>
	<p>Component separator Separates water from dry-wood.</p>	<p>Flash Pressure: 1atm Split fraction: 1 for water and 0 for dry-biomass in stream H₂O.</p>

Table 4-1: Aspen Unit Model Description (cont.)

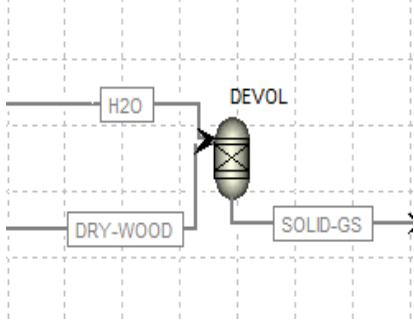
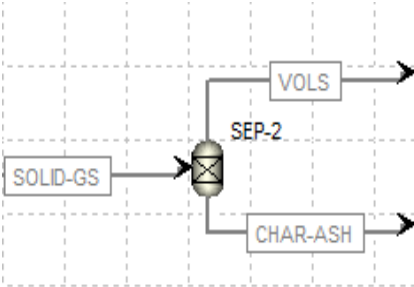
	<p>Yield reactor converts dry biomass + water into volatiles, char and ash.</p>	<p>Temperature: 673K Pressure: 1atm Yield: Volatiles: 84% Char: 15% Ash: 1%</p>
	<p>Component separator separates the volatiles from ash and char.</p>	<p>Flash Pressure: 1atm Split fraction: 1 for volatiles and 0 for ash and char in stream "vols".</p>

Table 4-1: Aspen Unit Model Description (cont.)

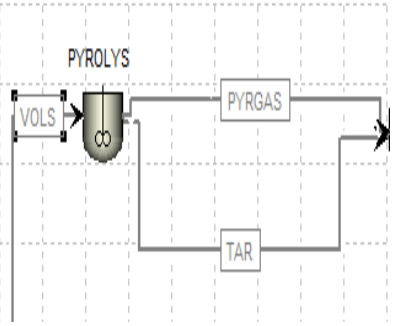
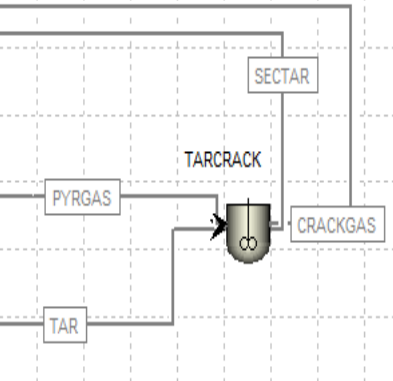
	<p>Kinetic CSTR is modeled with primary pyrolysis where the volatiles are decomposed to pyrgases and primary tar</p>	<p>Temperature: 673K Pressure: 1atm Reactions: primary pyrolysis</p>
	<p>Kinetic CSTR is modeled with tar cracking reaction where the primary tar formed in primary pyrolysis and decomposed to gases and secondary tar (benzene).</p>	<p>Temperature: 673K Pressure: 1atm Reactions: Tar Cracking</p>

Table 4-1: Aspen Unit Model Description (cont.)

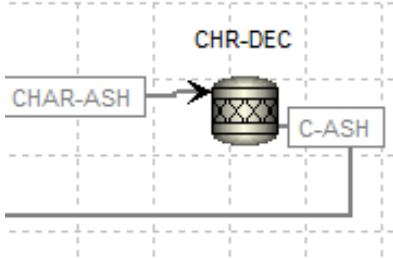
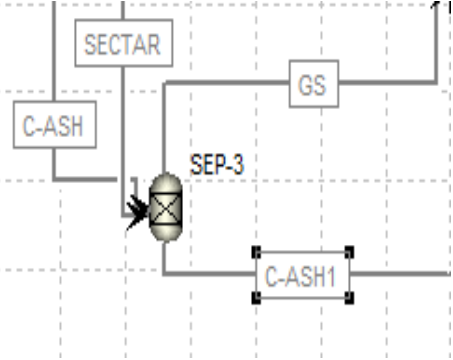
	<p>Decomposes char which is a non-conventional to carbon solid and other light gases present in char.</p>	<p>Pressure: 1atm Reactions: Char Decomposition</p>
	<p>Carbon and Ash formed from devolatilization and secondary tar are separated to a gas and a solid stream.</p>	<p>Flash Pressure: 1atm Split fraction: 1 for light gases in GS stream and 0 for ash, C (Solid) and Secondary tar in stream "C-ASH1".</p>

Table 4-1: Aspen Unit Model Description (cont.)

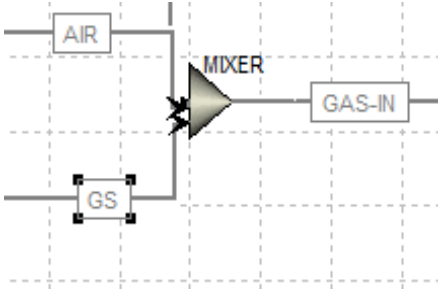
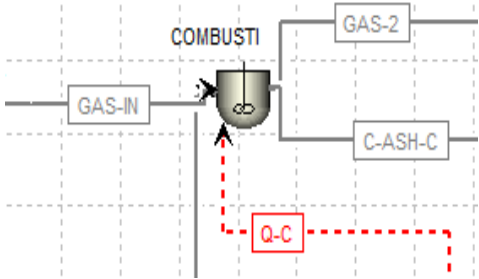
	<p>Mixes incoming oxygen with other gas stream split from the splitter from pyrolysis and char decomposition to be used as fuel for combustion zone.</p>	<p>Pressure: 1atm Valid phase: vapor</p>
	<p>Kinetic CSTR is modeled with a set of combustion reactions.</p>	<p>Pressure: 1atm Duty: Q-C Reactions: Combustion & Tar Cracking</p>

Table 4-1: Aspen Unit Model Description (cont.)

	<p>Kinetic CSTR is modeled with a set of gasification reactions.</p>	<p>Pressure: 1atm Duty: Q-G Reactions: Gasification Reactions</p>
--	--	---

5. MODEL VALIDATION, RESULTS AND DISCUSSION

Statistician George box wrote “All models are wrong but some are useful”. Therefore performance of any model will be based on how accurately the model predicted values are close to the real experimental data. Before we present our results, first step is to validate the syngas composition results from Aspen model with yield data from real systems. We have validated our results with Jeya Singh’s published work on downdraft gasifiers. Comparison between experimental results of Jeya Singh’s work with previously published experimental work on downdraft biomass gasifier is shown in Figure 5-1. We made use of this data to validate our model.

Mole fraction of carbon monoxide shown in Figure 5-1 is between eighteen to twenty percent which is exactly the range our model predicted shown in Figure 5-2. Experimental results show that mole fraction of hydrogen is between fifteen to twenty percent while our model predicted hydrogen to be little less than fifteen percent. Carbon Dioxide, methane and nitrogen experimental results match with aspen model predicted values. Hence we conclude that this aspen model developed is an acceptable representation of real biomass gasification system.

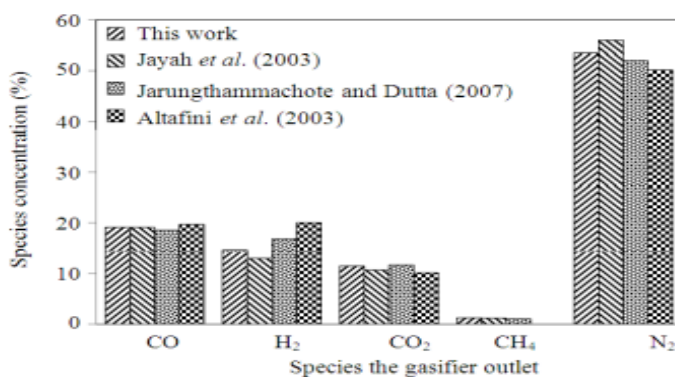


Figure 5-1: Various Experimental Results

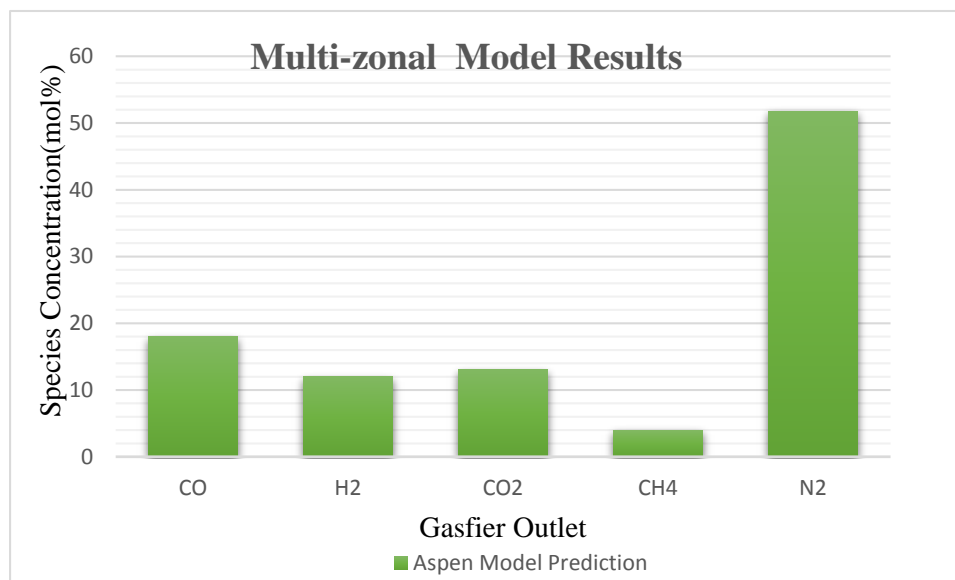


Figure 5-2: Aspen Model Results

Results are presented in 3 sections for three different types of feed introduced before. In each section process parameter and feedstock parameter are identified and optimized. Since the quality of syngas is defined based on the concentration of H₂ and CO, the optimum temperature is chosen as the point where the highest production of hydrogen and carbon monoxide is achieved with priority of hydrogen. For this reason, it is first shown how the quality of produced syngas changes with the temperature of gasification zone. Then based on this gasification temperature, the corresponding combustion temperature and air flow are found. Finally temperatures of different zones inside the reactor are shown for the chosen optimum point.

Pellets (8% moisture): The variation of gas yields with gasification temperature is shown in Figure 5-3. According to Ajay & David, at temperatures above 800 C, due to the endothermic nature of water gas shift reaction and dominance of Boudouard reaction,

hydrogen and carbon monoxide production increases. At high temperature, tar cracking also contributes to high gas yield. It is shown in Figure 5-3 that mole fraction of hydrogen and carbon monoxide goes up with increase in gasification temperature till 1200 K above which there is a decline in hydrogen formation. Multi-zonal model exactly tries to explain this particular fact. The temperature is directly related to the oxygen flow rate and at higher temperature carbon dioxide and water production goes up.

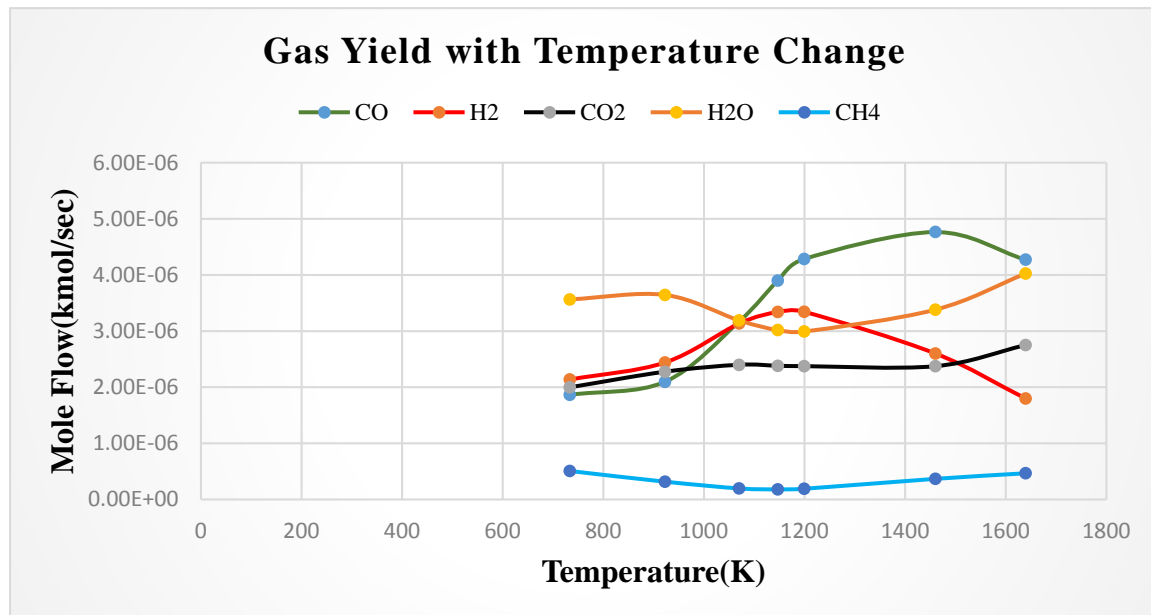


Figure 5-3: Gas Yield with Change in Temperature

It is observed in Figure 5-4 that the optimum point is at 1199 K where there is 25% H₂ and 32% CO in produced gas. Bed temperatures inside the reactor changes with the

change in air flow. As air flow into the reactor increases, the temperature in gasification and combustion bed increases as shown in Figure 5-4.

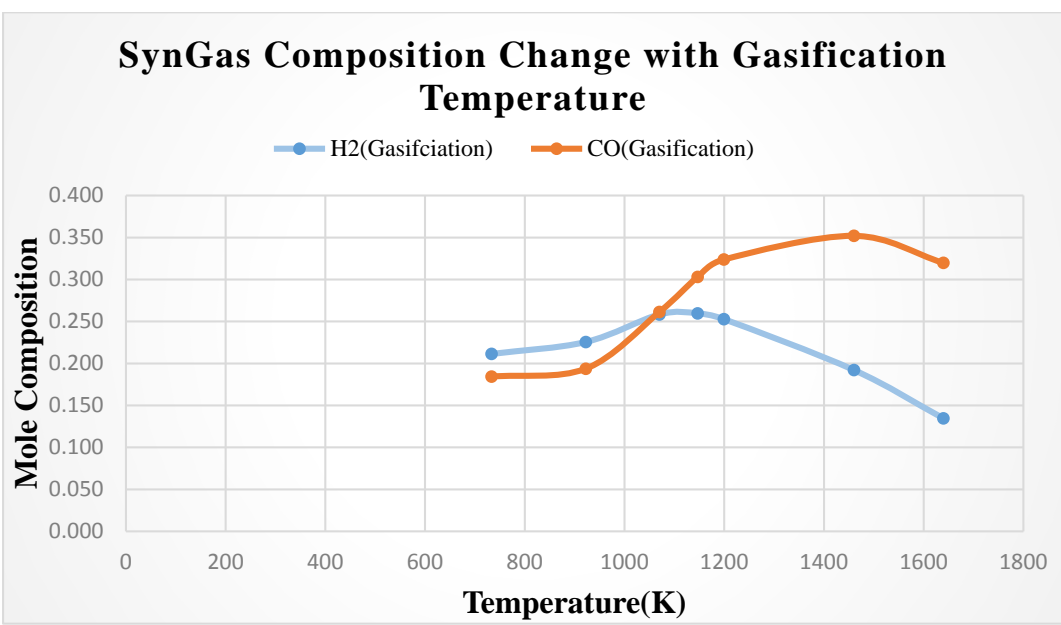


Figure 5-4: Syngas composition vs temperature for pellets

Based on the optimum temperature found from Figure 5-4, the corresponding combustion temperature and oxygen flow rate are found to be 1522 K and 0.25 kg/hr respectively from Figure 5-5.

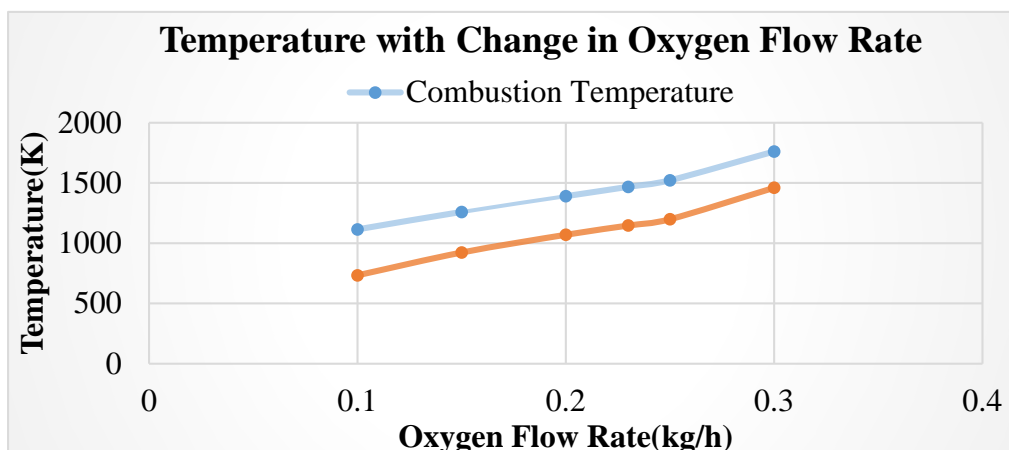


Figure 5-5: Temperature vs oxygen flow rate

Temperature for different zones for pellets in the reactor is shown in Figure 5-6.

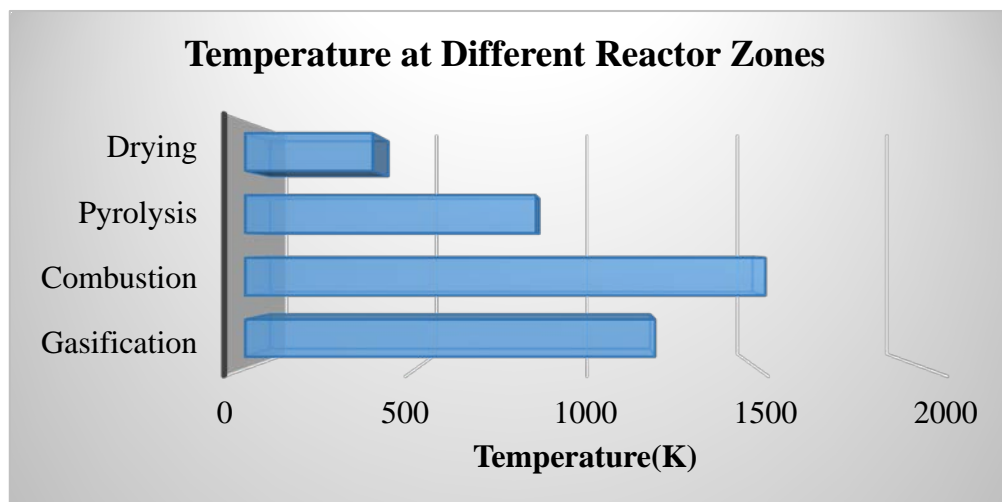


Figure 5-6: Temperature profile for pellet feed

As mentioned before, the temperature in drying and pyrolysis zone is fixed at 373 K and 850 K respectively. This is because at those temperatures maximum amount of water is removed from the raw feed in drying zone and also maximum conversion is achieved in pyrolysis reaction.

Flakes (20% moisture): It is observed in Figure 5-7 that the optimum gasification temperature is at 1226 K where there is 23% H₂ and 27% CO in produced gas. The quality of syngas has decreased for flakes which has a higher moisture content than pellets.

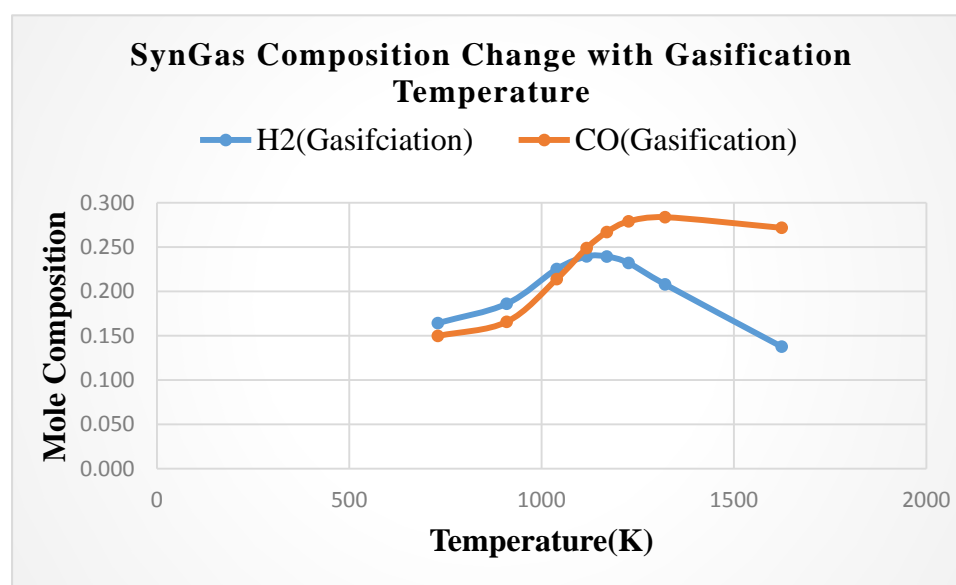


Figure 5-7: Syngas composition vs temperature for flakes

The corresponding oxygen flow rate is 0.27 kg/h and combustion temperature is 1551 K from Figure 5-8.

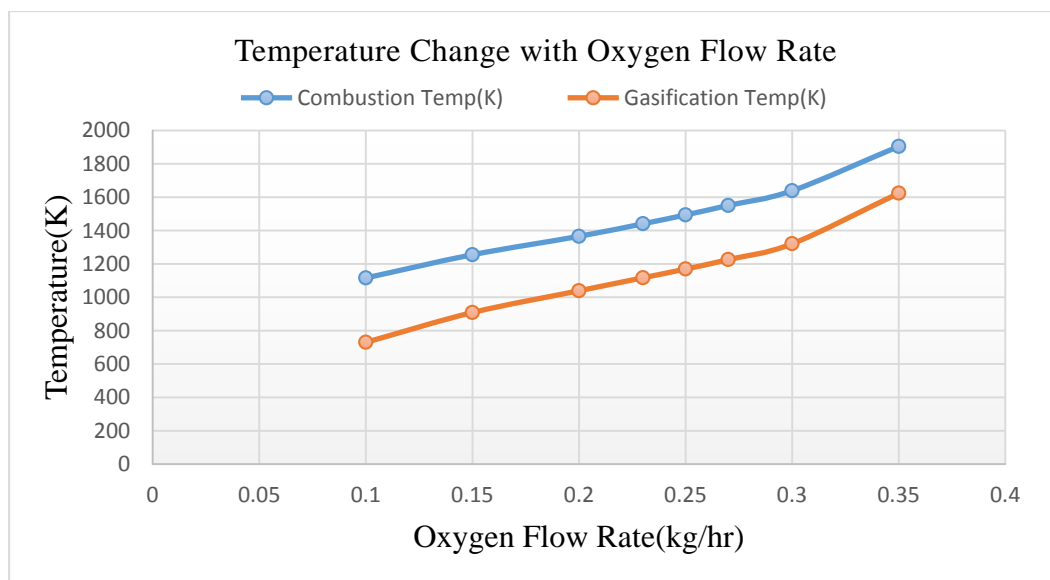


Figure 5-8: Temperature vs oxygen flow rate for flakes

The temperature for different zones for flakes inside the reactor is shown in Figure 5-9. Flakes has slightly higher temperature at the combustion zone and gasification zone compared to pellets.

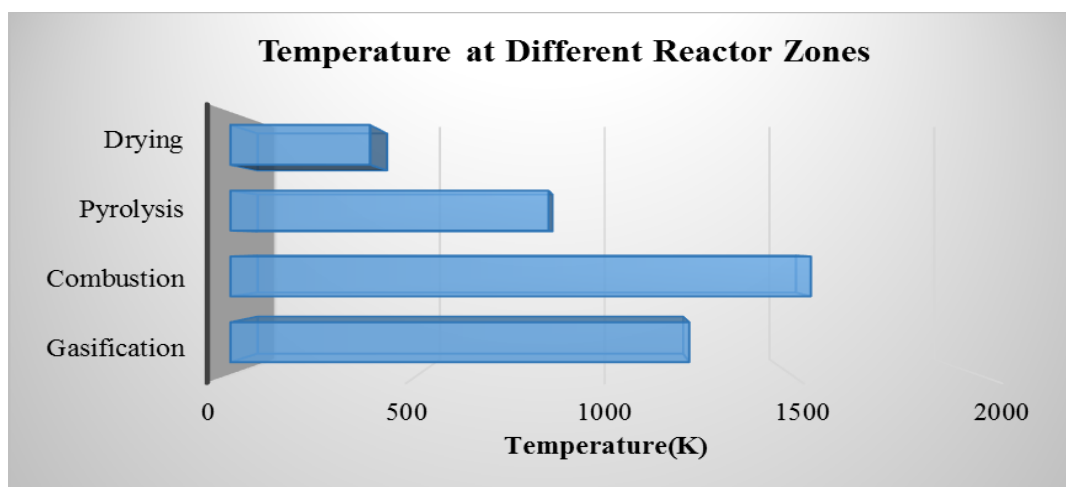


Figure 5-9: Temperature profile for flakes feed

Chips (35% moisture):It is observed in Figure 5-10 that the optimum gasification temperature is at 1145 K where there is 20% H₂ and 15% CO in produced gas. The quality of syngas keeps decreasing with increasing moisture content.

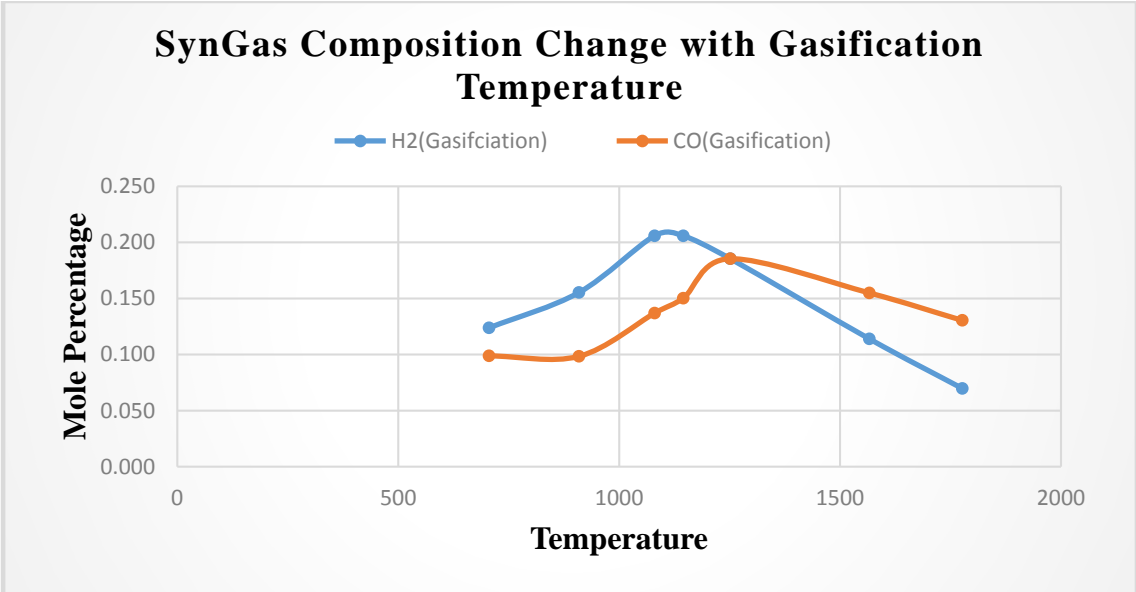


Figure 5-10: Syngas composition vs temperature for chips

The corresponding oxygen flow rate is 0.22 kg/h and combustion temperature is 1470 K is shown in Figure 5-11.

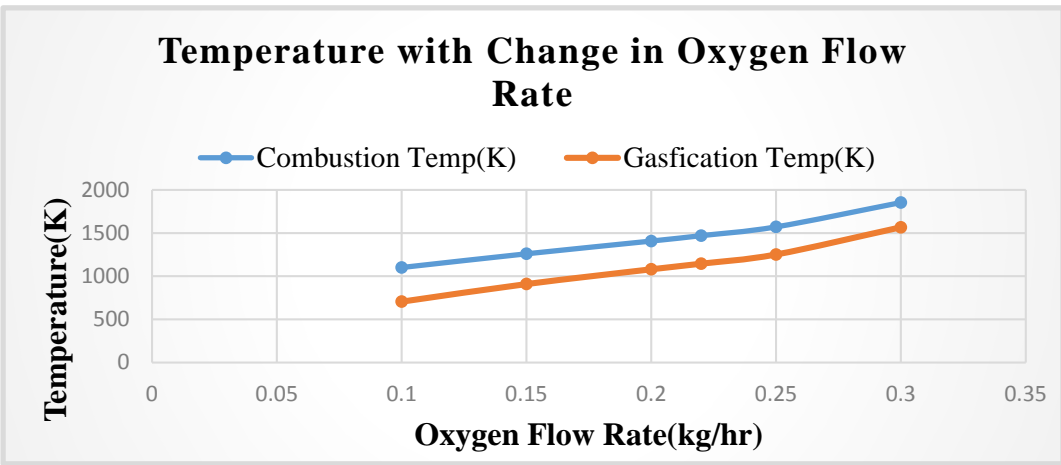


Figure 5-11: Temperature vs Oxygen flow rate for chips

The temperature for different zones for chips inside the reactor is shown in Figure 5-12. Chips has lower temperature in combustion and gasification zone comparing to pellets and flakes.

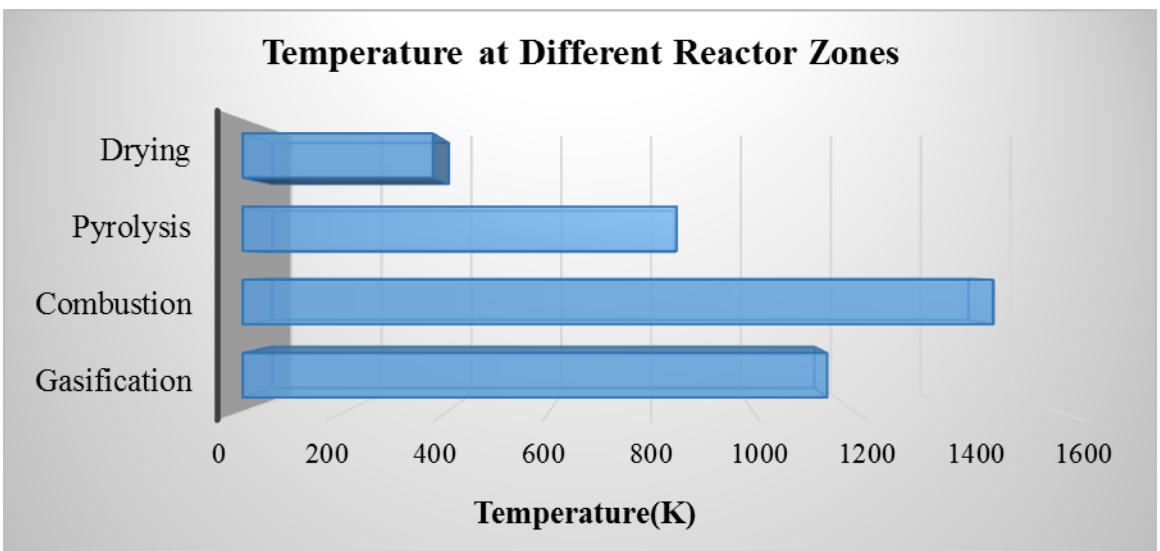


Figure 5-12: Temperature profile for chips

6. CONCLUSION

Multi-zonal modeling procedure for a downdraft biomass gasifier allows us to model different reactor zones in detail. Drying zone is modeled using a yield reactor which removes free water from biomass. Three steps devolatilization model which includes primary devolatilization, pyrolysis and tar cracking is modeled as a part of pyrolysis zone. All three reactions are modeled at same temperature. Combustion reactions are a combination of char oxidation reactions and volatile combustion reaction. Tar cracking conversion happens at higher temperature. So it is also specified at combustion zone. Gasification zone is modeled primarily with char gasification reactions along with water gas shift reaction. Multizonal modeling approach identified the critical impact of gasification temperature on syngas composition. Results show that at low temperature, the amount of CO/H₂ produced is less and at high temperatures (above 1300 K) combustion happens in gasification zone leading to less quality syngas.

This model identified that oxygen used determines the products and temperatures of reaction. Oxygen consumed is plotted against gasification temperature. Syngas production is plotted against gasification temperature to accurately predict the optimum gasification temperature. Moisture content in biomass is an important factor which determines the quality of syngas in down-draft gasifier. Effect of moisture content is studied using proximate and ultimate analysis of various feeds available at Missouri S&T Energy Center. Model predicted that pellet feed having low moisture content produced a syngas with higher CO/H₂ ratio while feed chips having higher moisture content produced low quality syngas which was the same case seen during the downdraft gasifier run in Energy Center lab.

REFERENCES

- [1] Schill, S. R. (2009, September 19). *IEA Task40: Biomass provides 10 percent of global energy use*. Retrieved from Biomass magazine: http://biomassmagazine.com/authors/view/Sue_Retka%20Schill.
- [2] *Renewable energy statistics*. (2015, May). Retrieved from EuroStat Statistics Explained: http://ec.europa.eu/eurostat/statistics-explained/index.php/Renewable_energy_statistics.
- [3] *Engineering International: the CIGR Ejournal*. Edenhofer, O., Madruga, R. P., & Sokona, Y. (2012). *Renewable Energy Sources and Climate Change Mitigation*. Cambridge: CAMBRIDGE UNIVERSITY PRESS.
- [4] Hegar, G. (n.d.). *Texas Renewable Energy Resource Assesement 2008*. Retrieved from State Energy Conservation Office: <http://www.seco.cpa.state.tx.us/publications/renewenergy/acknowledgements.php>.
- [5] Chopra, S., & Jain, A. (2007). A Review of Fixed Bed Gasification Systems for Biomass . *Agricultural Engineering International: the CIGR Ejournal*.
- [6] Fisher, B., Gagnon, D., & Sutcliffe, D. (2011). *Gasifier Powered Go-Kart*. Retrieved from <http://engin1000.pbworks.com/w/page/18942701/Gasifier%20Go-Kart>.
- [7] Food and Agriculture organization of United Nations. (1986). *Wood Gas as Engine Fuel*. Rome.
- [8] Tanger, P., Field, J. L., Jahn, C. E., Defoort, M. W., & Leach, J. E. (2013). Biomass for thermochemical conversion: targets and challenges. *Frontiers in PLANT SCIENCE*.
- [9] McGowan, T. F., Brown, M., Bulpitt, W., & Walsh, J. (2009). *Biomass and Alternate Fuel Systems: An Engineering and Economic Guide*. Wiley.
- [10] Vreugdenhil, B. J., & Zwart, R. W. (2009). *Tar formation in pyrolysis and gasfication*. Energy Research Centre of Netherlands.
- [11] Wu, Y., Zhang, Q., Yang, W., & Blasiak, W. (2013). Two Dimensional Computational Fluid Dynamic Simulation of Biomass Gasfication in a Downdraft Fixed-Bed Gasfier with Highly Preheated Air and Steam. *Energy & Fuels*.
- [12] Bhavanam, A., & Sastry, R. (2011). *Biomass Gasification Processes in Downdraft Fixed Bed Reactors: A Review*. International Journal of Chemical Engineering and Applications.

- [13] Worley, M., & Yale, J. (2012). *Biomass Gasification Technology Assessment*. Atlanta: National Energy Renewable Laboratory.
- [14] Martineza, J. D., Mahkamove, K., Andradeb, R. V., & Lorab, E. S. (2011). Syngas production in downdraft biomass gasifiers and its application using internal combustion engines. *Elsevier*.
- [15] Babu, B., & Sheth, P. (n.d.). Modeling and Simulation of Reduction Zone of Downdraft Biomass Gasifier: Effect of Air to Fuel Ratio.
- [16] AspenTech. (2011). Model for Moving Bed Coal Gasifier.
- [17] Kumar, A., Jones, D., & Hanna, M. (2009). Thermochemical Biomass Gasification: A Review of the Current Status of the Technology. *Energies*.
- [18] Singh, C. J., Sekhar, S. J., & K, T. (2014). Performance studies on downdraft gasifier with biomass energy sources available in remote villages. *American Journal of Applied Sciences*.

SECTION

2. CONCLUSIONS

Aspen Simulation with rigorous kinetic multi-zonal models have been developed for both process which can be modified for different operating facilities. Model allows investigation of various conditions difficult to test in lab to identify optimal process conditions. It is recommended to use Aspen models to conduct similar analysis for process design to establish system operating conditions.

Oil shale model showed the impact of temperature on pyrolysis reaction and further allowed us to do a technical optimization based on flow rate and temperature. Biomass gasification model showed the critical impact of gasification temperature on syngas composition, effect of oxygen on predicting the products/temperatures of reaction and finally the effect of moisture content on syngas composition.

Future work can be to perform a techno-economic analysis of both models. Future plan is to integrate biomass gasifier model with anaerobic digester or refinery Aspen model which will constitute and be a part of hybrid energy system.

APPENDIX

Fortran Codes developed by Aspen Technology used in these models.

1. Biomass Gasification Reactions

```
IMPLICIT NONE
```

```
C
```

```
C  DECLARE VARIABLES USED IN DIMENSIONING
```

```
C
```

```
    INTEGER NSUBS, NINT,  NPO,  NIWORK, NWORK,
```

```
    +   NC,  NR,  NTCAT, NTSSAT, NCOMP,
```

```
    +   NRALL, NUSERV, NINTR, NREALR, NIWR,
```

```
    +   NWR
```

```
C
```

```
#include "ppexec_user.cmn"
```

```
    EQUIVALENCE (RMISS, USER_RUMISS)
```

```
    EQUIVALENCE (IMISS, USER_IUMISS)
```

```
#include "dms_ncomp.cmn"
```

```
#include "rxn_rcstr.cmn"
```

```
#include "rxn_rprops.cmn"
```

```
    EQUIVALENCE (TEMP, RPROPS_UTEMP )
```

```
    EQUIVALENCE (PRES, RPROPS_UPRES )
```


EQUIVALENCE (VFRAC, RPROPS_UVFRAC)

EQUIVALENCE (BETA, RPROPS_UBETA)

EQUIVALENCE (VVAP, RPROPS_UVVAP)

EQUIVALENCE (VLIQ, RPROPS_UVLIQ)

EQUIVALENCE (VLIQS, RPROPS_UVLIQS)

EQUIVALENCE (B(1), IB(1))

C

#include "pputl_ppglob.cmn"

#include "dms_maxwrt.cmn"

#include "dms_plex.cmn"

C DECLARE ARGUMENTS

C

INTEGER IDXSUB(NSUBS), ITYPE(NSUBS), INT(NINT), IDS(2),
 + NBOPST(6,NPO), IWORK(NIWORK), IDX(NCOMP), INTR(NINTR),
 + IWR(NIWR), NREAL, KCALL, KFAIL,
 + KFLASH, NRL, NRV, I,
 + IMISS, KDIAG, KV, KER,
 + DMS_IFCMNC, LMW, LMWI

C

REAL*8 SOUT(1), WORK(NWORK), STOIC(NC,NSUBS,NR),
 + RATES(1), FLUXM(1), FLUXS(1), RATCAT(NTCAT),
 + RATSSA(NTSSAT),Y(NCOMP), X(NCOMP), X1(NCOMP),

+ X2(NCOMP)

C

REAL*8 RATALL(NRALL), USERV(NUSERV), REALR(NREALR),

+ WR(NWR), RATEL(1), RATEV(1), XCURR,

+ XMW(NCOMP_NCC),B(1), TEMP, PRES,

+ RGAS

C

REAL*8 REAL(NREAL), RMISS, XLEN, DIAM,

+ VFRAC, BETA, VVAP, VLIQ,

+ VLIQS, VMXV, DVMX

C

REAL*8 NCARIN, NCARGF, NO2, NCO,

+ NH2, NCO2, NH2O, NCH4,

+ NN2, NH2S, NC6H6, NTOTG,

+ NCARB, NSULF, MASH, YO2,

+ YCO, YH2, YCO2, YH2O,

+ YCH4, YN2, YH2S, YC6H6,

+ YASH

C

REAL*8 CCARB, CO2, CH2, XC,

+ DP, VOID, RHOCOA, VBED

C

REAL*8 PO2, PCO, PH2, PCO2,

```

+   PH2O,    PCH4,    PN2,    PH2S,
+   PC6H6,    PAMBI,    PT,    T,
+   PH2OEQ,    PCO2EQ,    PH2EQ

```

C

```

REAL*8 RCR,    Z,    FW,    E,
+   KFILM,    KASH,    KOVER,    K,
+   KH2O2,    RCARO2,    RCARH2O,    RCARCO2,
+   RCARH2,    RH2O2,    RCOH2O

```

```
NCARIN = REALR(1)
```

```
NCARGF = REALR(2)
```

```
MASH = REALR(3)
```

```
YASH = REALR(4)
```

```
RHOCOA = REALR(5)
```

C BED VOID FRACTION

```
VBED = RCSTRR_VFRRC
```

C DECLARE CONSTANT PARAMETERS: RGAS (CAL/MOL/K), PAMBI (ATM).

```
RGAS = 1.987D0
```

```
PAMBI = 1.01325D5
```

C RETRIVE MOLECULAR WEIGHT OF EACH COMPONENT (KG/KMOL)

LMW = DMS_IFCMNC('MW')

DO I = 1, NCOMP_NCC

LMWI = LMW+I

XMW(I) = B(LMWI)

END DO

C RETRIEVE TEMPERATURE(K), PRESSURE(ATM), MOLE FLOWS OF
COMPONENTS (KMOL/S).

T = SOUT(IDXSUB(1)-1+NCOMP_NCC+2)

PT = RPROPS_UPRES / PAMBI

NO2 = SOUT(IDXSUB(1)-1+1)

NCO = SOUT(IDXSUB(1)-1+2)

NH2 = SOUT(IDXSUB(1)-1+3)

NCO2 = SOUT(IDXSUB(1)-1+4)

NH2O = SOUT(IDXSUB(1)-1+5)

NCH4 = SOUT(IDXSUB(1)-1+6)

NN2 = SOUT(IDXSUB(1)-1+7)

NH2S = SOUT(IDXSUB(1)-1+8)

NC6H6 = SOUT(IDXSUB(1)-1+9)

NCARB = SOUT(IDXSUB(2)-1+10)

NSULF = SOUT(IDXSUB(2)-1+11)

NTOTG = NO2+NCO+NH2+NCO2+NH2O+NCH4+NN2+NH2S+NC6H6

C CALCULATE COMPONENT MOLE FRACTIONS

$$Y_{O_2} = N_{O_2} / N_{TOTG}$$

$$Y_{CO} = N_{CO} / N_{TOTG}$$

$$Y_{H_2} = N_{H_2} / N_{TOTG}$$

$$Y_{CO_2} = N_{CO_2} / N_{TOTG}$$

$$Y_{H_2O} = N_{H_2O} / N_{TOTG}$$

$$Y_{CH_4} = N_{CH_4} / N_{TOTG}$$

$$Y_{N_2} = N_{N_2} / N_{TOTG}$$

$$Y_{H_2S} = N_{H_2S} / N_{TOTG}$$

$$Y_{C_6H_6} = N_{C_6H_6} / N_{TOTG}$$

C CALCULATE COMPONENT PARTIAL PRESSURES(ATM)

$$P_{O_2} = Y_{O_2} * P_T$$

$$P_{CO} = Y_{CO} * P_T$$

$$P_{H_2} = Y_{H_2} * P_T$$

$$P_{CO_2} = Y_{CO_2} * P_T$$

$$P_{H_2O} = Y_{H_2O} * P_T$$

$$P_{CH_4} = Y_{CH_4} * P_T$$

$$P_{N_2} = Y_{N_2} * P_T$$

$$P_{H_2S} = Y_{H_2S} * P_T$$

$$P_{C_6H_6} = Y_{C_6H_6} * P_T$$

C CARBON AND COEFFICIENT $Y=RC/R$

$$XC = 1.0 - NCARB/NCARIN$$

$$RCR = (NCARB/NCARGF)**0.333$$

C REACTION RATE OF SOLID AND GAS PHASES

C C + O2

C PARAMETER FOR CALCULATING RATIO OF CO TO CO2

$$Z = 2500.0D0*EXP(-6249.0D0/T)$$

C REACTION RATE (KMOL/S)

$$KFILM = 0.292D0*4.26D0*(T/1800.0D0)**1.75/(DP*T)$$

$$VOID = 0.75D0$$

$$KASH = KFILM * VOID**2.5 * RCR / (1.0D0-RCR)$$

$$KOVER = KFILM*KASH / (KFILM+KASH)$$

$$RCARO2 = KOVER * PO2 * 1.0D-3 / 1.0D-6 * (1.0D0-VBED)$$

$$+ *RCSTRR_VOLRC$$

C C + H2O

C CALCULATE CONCENTRATION OF CARBON (KMOL/M**3)

$$CCARB = NCARB / MASH * RHOCOA*YASH * (1.0-VBED)$$

C REACTION RATE (KMOL/S)

$$K = 930.0D0$$

$$E = 45000.0D0$$

$$PH2O_{EQ} = PH2 * PCO / \exp(17.29 - 16330.0D0 / T)$$

$$RCARH2O = K * \exp(-E/RT) * CCARB * (PH2O - PH2O_{EQ})$$

$$+ \quad * RCSTRR_VOLRC$$

$$C \quad C + CO2 \text{ (KMOL/S)}$$

$$K = 930.0D0$$

$$E = 45000.0D0$$

$$PCO2_{EQ} = PCO * PCO / \exp(20.92 - 20280.0D0 / T)$$

$$RCARCO2 = K * \exp(-E/RT) * CCARB * (PCO2 - PCO2_{EQ})$$

$$+ \quad * RCSTRR_VOLRC$$

$$C \quad C + H2 \text{ (KMOL/S)}$$

$$PH2_{EQ} = \sqrt{PCH4 / \exp(-13.43 + 10100.0D0 / T)}$$

$$RCARH2 = \exp(-7.087D0 - 8078.0D0 / T) * CCARB * (PH2 - PH2_{EQ})$$

$$+ \quad * RCSTRR_VOLRC$$

$$C \quad H2 + O2$$

$$C \quad \text{TOTAL MOLAR VOLUME OF GAS PHASE (M**3/KMOL)}$$

$$KDIAG = 4$$

$$KV = 1$$

CALL PPMON_VOLV(T,RPROPS_UPRES,Y,NCOMP,IDX,NBOPST,KDIAG,
+ KV,VMXV,DVMX,KER)

C MOLE CONCENTRATION (KMOL/M**3)

$$CO2 = YO2 / VMXV$$

$$CH2 = YH2 / VMXV$$

C REACTION RATE (KMOL/S)

$$KH2O2 = 8.83D5 * DEXP(-9.976D4/8.3145D0/T)$$

RH2O2 = KH2O2 * (CH2*1.0D3) * (CO2*1.0D3)
+ *1.0D-3 * VBED * RCSTRR_VOLRC

C CO+H2O (KMOL/S)

$$FW = 0.0084D0$$

RCOH2O = FW * 2.877D5 * DEXP(-27760.0D0/RGAS/T)
+ *(YCO*YH2O - YCO2*YH2/EXP(-3.6890+7234/1.8/T))
+ * PT**(0.5D0-PT/250.0D0) * DEXP(-8.91D0+5553.0D0/T)
+ * RHOCOA * YASH * (1.0D0 - VBED) * RCSTRR_VOLRC

C INITIALIZE RATES

DO 100 I = 1, NC

RATES(I) = 0D0

100 CONTINUE

C REACTION RATE OF COMPONENTS (KMOL/S)

RATES(1) = -RCARO2*(2.0+Z)/2.0/(1.0+Z) - RH2O2*0.5D0

RATES(2) = RCARO2*Z/(1.0+Z) + RCARH2O*1.0D0
 + +RCARCO2*2.0D0 - RCOH2O

RATES(3) = RCARH2O*1.0D0 - RCARH2 *2.0D0
 + +RCOH2O - RH2O2

RATES(4) = RCARO2 *1.0/(1.0+Z) - RCARCO2*1.0D0
 + +RCOH2O

RATES(5) = -RCARH2O*1.0D0 + RH2O2
 + -RCOH2O

RATES(6) = RCARH2 *1.0D0

RATES(7) = 0.0D0

RATES(8) = 0.0D0

RATES(9) = 0.0D0

RATES(NCOMP_NCC*2-1) = -RCARO2 *1.0D0 - RCARH2O*1.0D0
+ -RCARCO2*1.0D0 - RCARH2 *1.0D0
RATES(NCOMP_NCC*2) = 0.0D0

RETURN

END

Oil Shale Pyrolysis

1. IMPLICIT NONE
2. C
3. C DECLARE VARIABLES USED IN DIMENSIONING
4. C
5. INTEGER NSUBS, NINT, NPO, NIWORK, NWORK,
6. + NC, NR, NTCAT, NTSSAT, NCOMP,
7. + NRALL, NUSERV, NINTR, NREALR, NIWR,
8. + NWR
9. C
10. #include "ppexec_user.cmn"
11. EQUIVALENCE (RMISS, USER_RUMISS)
12. EQUIVALENCE (IMISS, USER_IUMISS)
13. #include "dms_ncomp.cmn"
14. #include "rxn_rcstrr.cmn"
15. #include "rxn_rprops.cmn"
16. EQUIVALENCE (TEMP, RPROPS_UTEMP)
17. EQUIVALENCE (PRES, RPROPS_UPRES)
18. EQUIVALENCE (VFRAC, RPROPS_UVFRAC)
19. EQUIVALENCE (BETA, RPROPS_UBETA)
20. EQUIVALENCE (VVAP, RPROPS_UVVAP)
21. EQUIVALENCE (VLIQ, RPROPS_UVLIQ)

```
22.  EQUIVALENCE (VLIQS, RPROPS_UVLIQS)
23.      EQUIVALENCE (B(1), IB(1)    )
24. C
25. #include "pputl_ppglob.cmn"
26. #include "dms_maxwrt.cmn"
27. #include "dms_plex.cmn"
28.
29. C  DECLARE ARGUMENTS
30. C
31.  INTEGER IDXSUB(NSUBS), ITYPE(NSUBS), INT(NINT), IDS(2),
32.  +   NBOPST(6,NPO), IWORK(NIWORK), IDX(NCOMP), INTR(NINTR),
33.  +   IWR(NIWR),  NREAL,    KCALL,  KFAIL,
34.  +   KFLASH,  NRL,    NRV,  I,
35.  +   IMISS,  KDIAG,  KV,  KER,
36.  +   DMS_IFCMNC, LMW,    LMWI
37. C
38.  REAL*8 SOUT(1),  WORK(NWORK), STOIC(NC,NSUBS,NR),
39.  +   RATES(1),  FLUXM(1),  FLUXS(1), RATCAT(NTCAT),
40.  +   RATSSA(NTSSAT),Y(NCOMP),  X(NCOMP), X1(NCOMP),
41.  +   X2(NCOMP)
42. C
43.  REAL*8 RATALL(NRALL), USERV(NUSERV), REALR(NREALR),
44.  +   WR(NWR),  RATEL(1),  RATEV(1), XCURR,
```

```
45. + XMW(1), B(1), TEMP, PRES
46. C
47. REAL*8 REAL(NREAL), RMISS, XLEN, DIAM,
48. + VFRAC, BETA, VVAP, VLIQ,
49. + VLIQS, VMXV, DVMX
50. C
51. REAL*8 FACTH2, FACTH2O, FACTH2S, FACTNH3, FACTCO,
52. + FACTCO2, FACTCH4, FACTC2H6, FACTC3H8, FACTC4H10,
53. + FACTOIL, FACTCHAR, FKO, CKO, T,
54. + FK, VBED, VOLR, K, RKEROGEN
55. C
56. REAL*8 RH2, RH2O, RH2S, RNH3, RCO,
57. + RCO2, RCH4, RC2H6, RC3H8, RC4H10,
58. + ROIL, RCHAR
59.
60.
61. C
62. C BEGIN EXECUTABLE CODE
63.
64. C-----
65. C INPUT DATA
66.
```

67. C STOICHIOMETRIC FACTOR FOR EACH PYROLYSIS COMPONENT
(KG EACH COMPONENT/KG KEROGEN)

68. $FACTH_2 = 0.0010$

69. $FACTH_2O = 0.0268$

70. $FACTH_2S = 0.0010$

71. $FACTNH_3 = 0.0010$

72. $FACTCO = 0.0057$

73. $FACTCO_2 = 0.0359$

74. $FACTCH_4 = 0.0142$

75. $FACTC_2H_6 = 0.0118$

76. $FACTC_3H_8 = 0.0117$

77. $FACTC_4H_{10} = 0.0117$

78. $FACTOIL = 0.4767$

79. $FACTCHAR = 0.4025$

80.

81.

82. C KEROGEN FLOW RATE (KG/S) AND CONCENTRATION (KG/M³
SHALES) IN ORIGINAL SHALE

83. $FKO = 0.0192$

84. $CKO = 323.66$

85. C-----

86.

87.

88. C RETRIEVE REACTION TEMPERATURE (K) AND LEFT KEROGEN
 FLOW RATE (KG/S)

89. T = SOUT(IDXSUB(1)-1+NCOMP_NCC+2)

90. FK = SOUT(IDXSUB(3)-1+1)

91.

92.

93. C RETRIEVE VOID FRACTION AND REACTOR VOLUME (M**3)

94. VBED = RCSTRR_VFRRC

95. VOLR = RCSTRR_VOLRC

96.

97.

98. C RETRIVE MOLECULAR WEIGHT OF EACH COMPONENT
 (KG/KMOL)

99. LMW = DMS_IFCMNC('MW')

100. DO I = 1,NCOMP_NCC

101. LMWI = LMW+I

102. XMW(I) = B(LMWI)

103. END DO

104.

105.

106. C TOTAL PYROLYSIS RATE OF KERGOEN (KG KEROGEN/M**3
 SHALE/S)

107. K = 6.9E10*EXP(-21790.0/T)

$$108. \quad \text{RKEROGEN} = K * \text{CKO} * (\text{FK}/\text{FKO})^{**1.4}$$

109.

110.

111. C REACTION RATE OF EACH COMPONENT (CONVENTIONAL:
KMOL/S; NONCONVENTIONAL: KG/S)

$$112. \quad \text{RH2} = \text{RKEROGEN} * \text{FACTH2} / \text{XMW}(3) * (1.0 - \text{VBED}) * \\ \text{VOLR}$$

$$113. \quad \text{RH2O} = \text{RKEROGEN} * \text{FACTH2O} / \text{XMW}(4) * (1.0 - \text{VBED}) \\ * \text{VOLR}$$

$$114. \quad \text{RH2S} = \text{RKEROGEN} * \text{FACTH2S} / \text{XMW}(6) * (1.0 - \text{VBED}) \\ * \text{VOLR}$$

$$115. \quad \text{RNH3} = \text{RKEROGEN} * \text{FACTNH3} / \text{XMW}(7) * (1.0 - \text{VBED}) \\ * \text{VOLR}$$

$$116. \quad \text{RCO} = \text{RKEROGEN} * \text{FACTCO} / \text{XMW}(9) * (1.0 - \text{VBED}) * \\ \text{VOLR}$$

$$117. \quad \text{RCO2} = \text{RKEROGEN} * \text{FACTCO2} / \text{XMW}(10) * (1.0 - \text{VBED}) \\ * \text{VOLR}$$

$$118. \quad \text{RCH4} = \text{RKEROGEN} * \text{FACTCH4} / \text{XMW}(11) * (1.0 - \text{VBED}) \\ * \text{VOLR}$$

$$119. \quad \text{RC2H6} = \text{RKEROGEN} * \text{FACTC2H6} / \text{XMW}(12) * (1.0 - \text{VBED}) \\ * \text{VOLR}$$

$$120. \quad \text{RC3H8} = \text{RKEROGEN} * \text{FACTC3H8} / \text{XMW}(13) * (1.0 - \text{VBED}) \\ * \text{VOLR}$$


```
121.          RC4H10  = RKEROGEN * FACTC4H10 / XMW(14) * (1.0-
          VBED) * VOLR
122.          ROIL   = RKEROGEN * FACTOIL  / XMW(15) * (1.0-VBED)
          * VOLR
123.          RCHAR  = RKEROGEN * FACTCHAR * (1.0-VBED) * VOLR
124.          RKEROGEN = -RKEROGEN * (1.0-VBED) * VOLR
125.
126.  C    WRITE(MAXWRT_MAXBUF(1),200) XMW(15)
127.  C 200 FORMAT(1X,"XMW=",F11.5)
128.  C    CALL DMS_WRTTRM(1)
129.
130.
131.  C  INITIALIZE RATES
132.      DO 100 I = 1, NC
133.          RATES(I) = 0D0
134.      100 CONTINUE
135.
136.
137.  C  REACTION RATE OF COMPONENTS
138.
139.  C  MIXED COMPONENTS
140.          RATES(1) = 0.0D0
141.
```

142. RATES(2) = 0.0D0
- 143.
144. RATES(3) = RH2
- 145.
146. RATES(4) = RH2O
- 147.
148. RATES(5) = 0.0D0
- 149.
150. RATES(6) = RH2S
- 151.
152. RATES(7) = RNH3
- 153.
154. RATES(8) = 0.0D0
- 155.
156. RATES(9) = RCO
- 157.
158. RATES(10) = RCO2
- 159.
160. RATES(11) = RCH4
- 161.
162. RATES(12) = RC2H6
- 163.
164. RATES(13) = RC3H8

165.
166. RATES(14) = RC4H10
167.
168. RATES(15) = ROIL
169.
170. C CISOLID COMPONENTS
171. RATES(NCOMP_NCC+16) = 0.0D0
172.
173. RATES(NCOMP_NCC+17) = 0.0D0
174.
175. RATES(NCOMP_NCC+18) = 0.0D0
176.
177. RATES(NCOMP_NCC+19) = 0.0D0
178.
179. RATES(NCOMP_NCC+20) = 0.0D0
180.
181. RATES(NCOMP_NCC+21) = 0.0D0
182.
183. RATES(NCOMP_NCC+22) = 0.0D0
184.
185. RATES(NCOMP_NCC+23) = 0.0D0
186.
187. RATES(NCOMP_NCC+24) = 0.0D0

```
188.  
189.          RATES(NCOMP_NCC+25) = 0.0D0  
190.  
191.          RATES(NCOMP_NCC+26) = 0.0D0  
192.  
193.    C  NONCONVENTIONAL COMPONENTS  
194.          RATES(NCOMP_NCC*2+1) = RKEROGEN  
195.  
196.          RATES(NCOMP_NCC*2+2) = RCHAR  
197.  
198.          RETURN  
199.    END
```

VITA

Anand Alembath was born on February 25, 1991 in Coimbatore (India). Anand earned his bachelor's degree in Chemical Engineering from Amrita Vishwa Vidyapeetham, Ettimadai. During this time, he found an opportunity to work under the VP of Kavin Engineering Sriprabu Ramamoorthy on process modeling and simulation. He completed his B.Tech degree in October of 2013.

Anand joined the graduate school Missouri University of Science and Technology in January of 2014 for a master's degree. There, he was given an opportunity to work as a graduate research assistant under Dr. Joseph Smith. He was also a graduate teaching assistant and course instructor during his time as a graduate student in the Chemical and Biochemical Engineering Department. Anand Alembath graduated with his M.S. in Chemical Engineering in May of 2016.